Please cite this article in press as: Feng et al., Chiral perovskites: From chirality mechanisms to photovoltaics, Matter (2026), https://doi.org/10.1016/j.matt.2026.102758

Matter

CellPress

Review

Chiral perovskites: From chirality mechanisms to photovoltaics

Yuyi Feng,[1,2] Yifan Zeng,[1] Xin Bi,[1] Yuxuan Dong,[1] Hao Wang,[1] Yanheng Wang,[1] Qingyun Zhu,[2] Jianyu Li,[1] Fangci Zhang,[1] Zhongrui Wang,[1] Chunhui Zhang,[1] Chenlei Jiang,[1] Clayton A. Nemitz,[3] and Meicheng Li[1,*]

[1]State Key Laboratory of Alternate Electrical Power System with Renewable Energy Sources, North China Electric Power University, Beijing 102206, China

[2]Qinghai Province Institute for Product Quality Inspection & Testing, Qinghai 810017, China

[3]Department of Physics and Astronomy, University of North Carolina, Chapel Hill, NC 27516, USA

*Correspondence: mcli@ncepu.edu.cn

https://doi.org/10.1016/j.matt.2026.102758

PROGRESS AND POTENTIAL Photovoltaics play a vital role in clean energy innovation. Perovskites have emerged as a cornerstone material for next-generation solar cells due to their exceptional optoelectronic properties, with power conversion efficiencies rising dramatically from 3.8% to 27.3%, approaching the theoretical limit. Due to their compositional and structural tunability, perovskites also serve as an excellent platform for introducing chirality. Chiral perovskites have demonstrated significant potential in various fields, including chiroptics and spin photonics. In recent years, phenomena such as the Rashba effect and chiral-induced spin selectivity in chiral perovskites have garnered considerable attention for their potential applications in photovoltaics.

This review first classifies the main types of chiral perovskites, then explores the functional mechanisms through which their distinctive properties enhance photovoltaic performance, and finally outlines current challenges and future research directions. The work aims to provide a structured reference for ongoing studies in this evolving field and inspire cross-disciplinary research at the intersection of chirality, materials, and energy.

SUMMARY

The integration of chiral perovskite architectures into photovoltaics has emerged as a burgeoning area of research. We first analyze the fundamental mechanisms inducing chirality in perovskite structures, revealing that various properties of chirality with distinct mechanisms enhance solar cell performance via reducing material defects, inhibiting carrier recombination, extending carrier lifetime, etc., especially through their synergistic interactions. Moreover, we discuss how the ferroelectric photovoltaic behavior of chiral perovskites could enable novel device paradigms, introducing the innovative concept of an "artificial ferroelectric domain wall based on chiral perovskites," which holds theoretical potential for achieving breakthrough photovoltages. Key current limitations are also addressed, alongside proposed solutions such as scalable synthesis of 3D chiral perovskites via crystal skeleton expansion. Promising future directions include AI-assisted metamaterial design for efficiency enhancement and development of integrated micro-devices leveraging multifunctional chiral perovskites. By connecting fundamental principles of chiral materials with practical photovoltaic implementation, this work offers both methodological perspectives and actionable strategies for advancing high-performance chiral perovskite solar cells.

INTRODUCTION

Recently, perovskites have attracted extensive attention because of their excellent photoelectric properties. Unique ABX_3 structure with adjustable compositions (A = larger organic/inorganic cations; B = smaller non-polar cations; X = oxygen ion or halogen ion) gives them the characteristics of large absorption coefficient,[1–3] high carrier mobility,[3–7] long carrier diffusion length,[8–10] designable crystal structure,[11–13] adjustable band gap,[14–17] etc. They are ideal materials for photovoltaic cells,[18–24] light-emitting diodes,[25–31] photodetectors,[32–34] lasers,[35–37] and other devices. Especially in photovoltaics, perovskite solar cells, as the third generation of solar cells, have attracted much attention and achieved excellent results: the best laboratory certification efficiency is as high as 27.3%.[38]

Please cite this article in press as: Feng et al., Chiral perovskites: From chirality mechanisms to photovoltaics, Matter (2026), https://doi.org/10.1016/j.matt.2026.102758

An object is chiral if it cannot coincide with its mirror image by translation and rotation.[39] Substances with microscopic chirality and their enantiomers often have very different physicochemical and biological properties. For example, some different enantiomers with the same molecular formula (such as D/L-tartaric acid) will deflect the linearly polarized light penetrating it in various directions, that is, demonstrate optical activity[40]; the right-hand isomer of the famous chiral drug thalidomide has excellent calming effects, while its left-handed isomer is responsible for more than 10,000 fetal malformations.[41] These differences make chirality widely used in various fields, resulting in the emergence of various chiral materials. Among them, perovskite has become one of the important carriers to introduce chirality because of its highly adjustable composition and structure as well as its relatively simple synthesis process. Chiral perovskites have the advantages of both chiral materials and perovskites, which have been widely used in chiral optics,[42,43] ferroelectricity,[44–46] spin photonics,[47,48] optoelectronics,[49–51] and other fields. However, specific analyses and summaries of the application potential of chiral perovskites in the photovoltaic field are lacking.

The main content of this review is shown in Figure 1. We first outline the primary mechanisms for inducing chirality in perovskites, including internal crystal ions, surface-bound ligands, and chiral nanostructures extending beyond the crystal scale. We then evaluate the theoretical foundations and practical approaches for deploying chiral perovskites in photovoltaic systems. Perovskite chirality can not only enhance photovoltaic performance through the Rashba effect and chiral spin-induced selectivity but also improve the stability and operational lifetime of perovskite photovoltaics via passivation and enhanced mechanical properties. Moreover, chiral perovskites show significant promise for novel photovoltaic devices, particularly in ferroelectric photovoltaics (FE-PVs), potentially overcoming the limitations of conventional devices and breaking the Shockley-Queisser limit. Within this discussion, we introduce two conceptual advances: the "multi-mechanistic role of chirality in perovskites" and the "chiral-perovskite-based ferroelectric domain wall." Finally, we address existing challenges including limited conversion efficiency and fragile stability in applying chiral perovskites to photovoltaic devices and propose future research directions. The intrinsic symmetry-breaking and multi-physical coupling (e.g., Rashba, chiral-induced spin selectivity [CISS] and ferroelectricity) in chiral perovskites offer a distinct materials platform to address these challenges via novel physical mechanisms, offering a consolidated reference for researchers in this evolving field.

CHIRALITY MECHANISMS IN PEROVSKITES

At present, there are many schemes to introduce chirality into perovskite materials. Essentially, these methods introduce symmetry breaking into perovskites. In this section, referring to and combining with the existing classification methods and further refining,[43,52] we classify the common mechanisms of chirality in perovskites into three categories: (I) internal ions of crystals; (II) chiral ligands on the crystal surface; (III) chiral nanostructures beyond the crystal level. These introduce symmetry breaking to perovskites at different scales: the first two at the scale of the crystal structure, the latter beyond the crystal structure. The following introduces the principles of the three mechanisms of chirality and classifies them in more detail.

Intracrystalline ions inducing chirality

A common mechanism of chirality in perovskites is the internal ions of crystals. In the standard 3D perovskite crystal structure (ABX_3), the smaller B-site cations are coordinated with six X-site anions to form $[BX]_6^{n-}$ octahedrons, while the larger A-site cations are embedded in the middle of eight $[BX]_n^{6-}$ octahedrons to coordinate with 12 X-site anions. The simplest method of obtaining chiral perovskites is replacing the A-site cations with other ions. According to the mechanism of chiral transfer, there are three main sources of chirality provided by this method: intrinsic chirality of ions; ion-induced crystal structure distortion; and electron interaction. The latter two often lead to asymmetries of crystal structure, such as Sohncke space groups.[43,53] For ease of understanding, this section divides the method into A-site substitution, A-site intercalation, and Jahn-Teller distortion according to different ions.

A-site substitution: by replacing the achiral A-site cations in the perovskites with chiral cations with equal charge and appropriate size, the perovskite can be made chiral. This method does not destroy the 3D crystal structure of perovskite, but preserves it. In general, the A-site chiral cations provide their intrinsic chirality, while inducing the surrounding $[BX]_n^{6-}$ octahedron to skew and deform through electron interactions (such as hydrogen bonds, etc.), further amplifying the chirality. This mechanism is very intuitive and easy to understand, but it is very rare because the chiral A-site cations are generally large and difficult to confine to the classical 3D perovskite crystal structure. Specifically, R/S/rac-3AP-NH_4X_3 and R/S/rac-3AQ-NH_4X_3 (X = Cl or Br, 3AP = 3-ammoniopyrrolidinium, 3AQ = 3-ammonioquinuclidinium) are the few A-site substituted perovskites with classical 3D crystal structure which are also good ferroelectrics and rare non-metallic perovskites (Figure 2A), with great potential in FE-PVs and green perovskites[54]; Theoretically, based on structural optimization, phonon spectrum, formation energy, and *ab initio* molecular dynamics simulations, Long et al.[60] believed that the chirality of chiral cations can be successfully transferred to the framework of 3D hybrid organic-inorganic perovskites (HOIPs), and the resulting 3D chiral HOIPs have good kinetic and thermodynamic properties. In addition, some recent studies have taken a novel approach to substituting A-site for chiral 3D perovskites by breaking the classical perovskite 3D structure; for example, each A-site ion of (R/S-PyEA)Pb_2Br_6 (PyEA = (R/S)-1-(pyridine-4-yl)ethan-1-amine) is embedded between 12 $[PbBr]_6^{n-}$ octahedra instead of 8 (Figure 2B).[55] On that basis, more complex chiral 3D perovskite designs, such as $(R/S\text{-}3APr)_2Pb_4I_{12}\cdot 2H_2O$ (R/S-3APr = R/S-3-aminopyrrolidine),[61] (R/S-BPEA)$EA_6Pb_4Cl_{15}$ (R/S-BPEA = (R/S)-1-4 bromophenylethylamine, EA = ethylamine),[56] combine chiral and achiral A-site ions (Figure 2C). In general, the A-site replacement of perovskite with classical 3D crystal structure is difficult to achieve due to limitations on the volume of A-site ions, but special-shaped 3D perovskite crystal structures that break through the traditional strategy open up new possibilities for the realization of A-site ion replacement 3D perovskite.

Please cite this article in press as: Feng et al., Chiral perovskites: From chirality mechanisms to photovoltaics, Matter (2026), https://doi.org/10.1016/j.matt.2026.102758

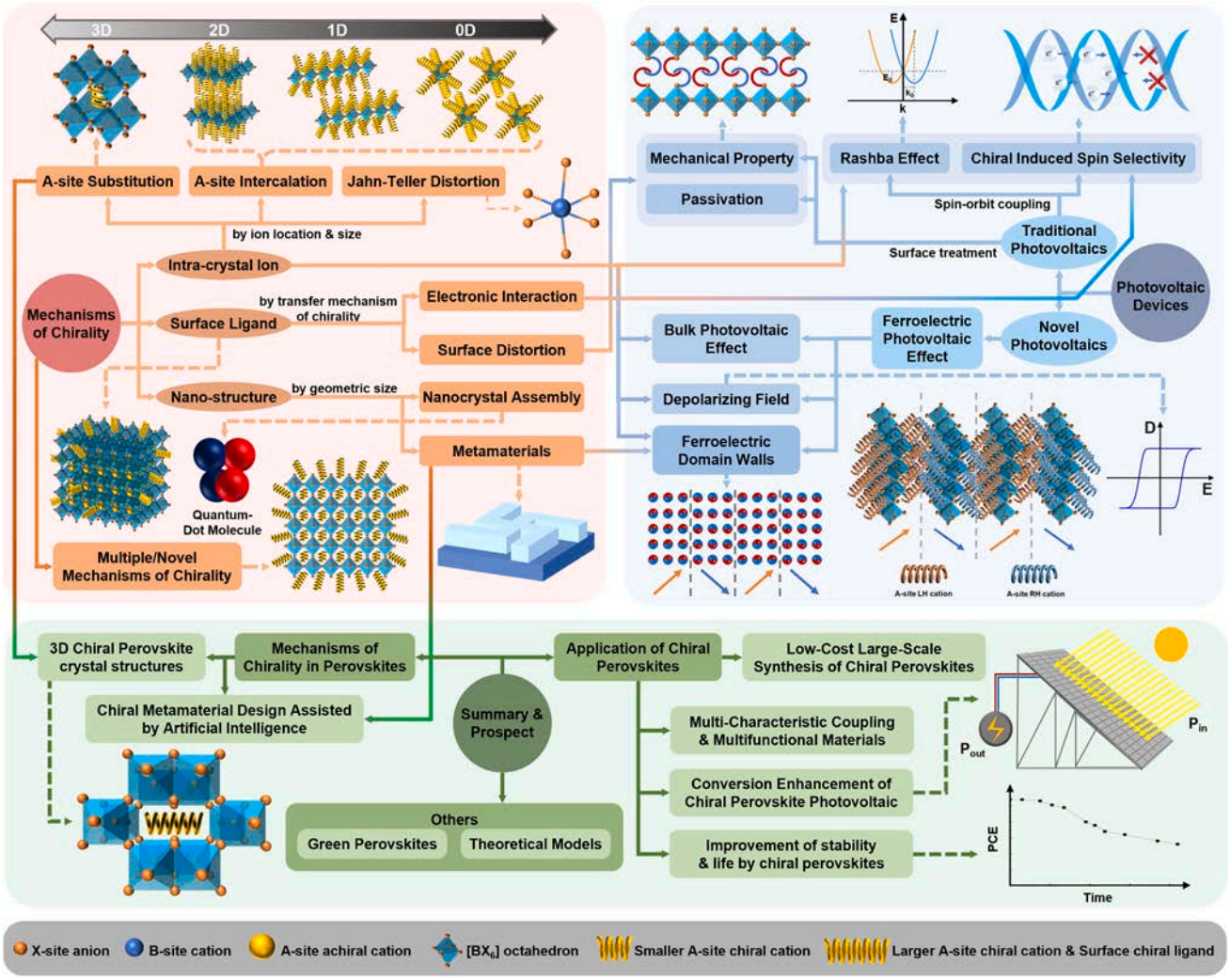

Figure 1. Schematic diagram of the review, the dotted lines show the example diagram, and the gradient lines show the connection between the different parts

A-site intercalation: when the chiral cations occupying the A-site are too large to be accommodated in the space between the eight $[BX]_6^{n-}$ octahedrons, the classical 3D perovskite crystal structure will be destroyed. Depending on the chiral cation, 2D, 1D, and 0D chiral perovskites will be generated.[62] The earliest such chiral perovskites appeared in 2003, when S/R-MBA was used to replace the original A-position cations, and corresponding 1D and 2D chiral perovskites were successfully prepared (Figure 2D).[57,58] In such low-dimensional chiral perovskites, because the proportion of chiral A-site ions is significantly higher than that of 3D perovskites, they often show higher chirality.[63] In addition, even if some large organic cations occupying the A position do not possess intrinsic chirality, synthetic organic inorganic hybrid perovskites may also possess chirality, which is related to the Sohncke space group. For example, $(piperidinium)_2SbCl_5$ (the A-site ion is an achiral chair piperidinium) with chirality has the space group $P2_12_12_1$, which belongs to the non-centrosymmetric Sohncke space group[64]; on the other hand, it may be related to the structure of chiral macromolecules themselves. For example, although the A-site ion cystamine in $CystaH_2[CuCl_4]$ does not have intrinsic chirality, it has a long chain structure, and will be twisted into a chiral helical structure under the influence of an external electric field.[65]

Jahn-Teller distortion: unlike the lattice structure deformation caused by A-site cations mentioned above, it is possible to induce Jahn-Teller distortion when certain cations are used to replace B-site cations in perovskite. In a crystal, the asymmetric occupation of electrons in degenerate orbitals will lead to the distortion of the crystal geometry, which will reduce the symmetry of the crystal and the degeneracy of the orbital, and further reduce the energy of the system. Electron asymmetry in degenerate orbitals has special requirements for the extranuclear electron configuration of B-site cations. Currently, B-site cations that can induce Jahn-Teller distortion include Cu^{2+},[59,66] Cr^{2+}/Cr^{3+},[67] Fe^{2+}/Fe^{3+},[67] Mn^{3+},[68] etc. Although these Jahn-Teller ions do not possess intrinsic chirality, their induced lattice

Please cite this article in press as: Feng et al., Chiral perovskites: From chirality mechanisms to photovoltaics, Matter (2026), https://doi.org/10.1016/j.matt.2026.102758

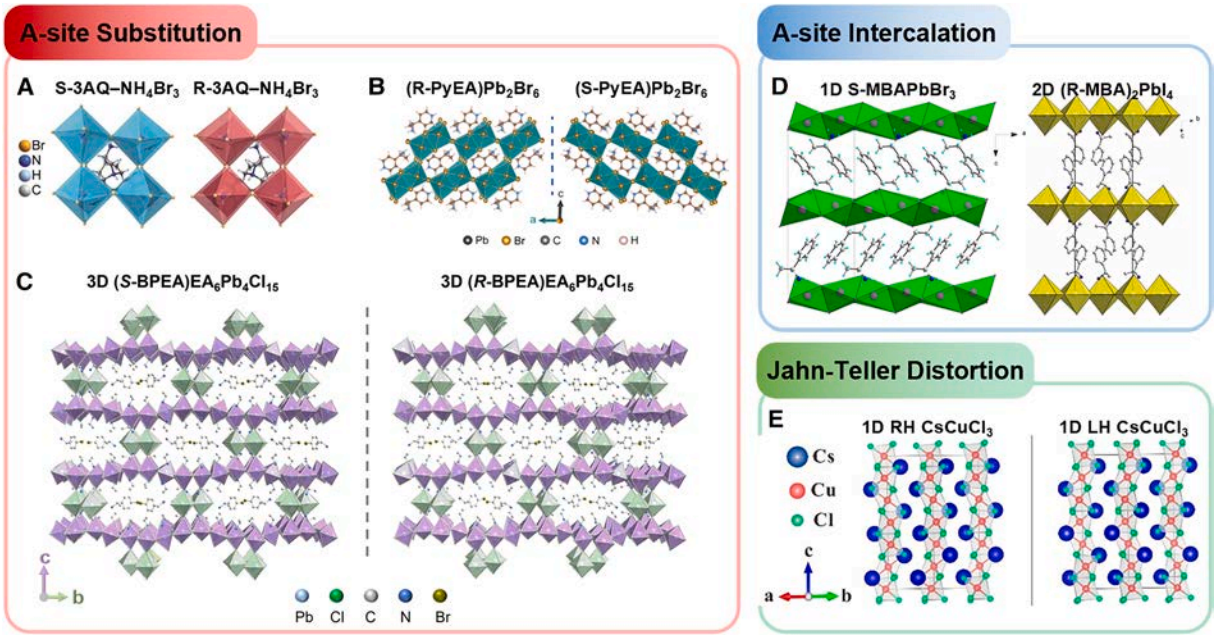

Figure 2. Chiral perovskite crystal structure diagram

(A) Traditional chiral 3D perovskite crystal structure, S/R-3AQ-NH_4Br_3 as examples, reproduced with permission from Ye et al.,[54] AAAS.

(B and C) Special-shaped chiral 3D perovskite crystal structure, (R/S-PyEA)Pb_2Br_6 and (S/R-BPEA)$EA_6Pb_4Cl_{15}$ as examples, reproduced with permission from Bai et al. and Guan et al.,[55,56] ACS and Wiley-VCH.

(D) S-$MBAPbBr_3$ chiral 1D perovskite on the left, reproduced with permission from Billing and Lemmerer,[57] International Union of Crystallography; $(R\text{-}MBA)_2PbI_4$ chiral 2D perovskite on the right, reproduced with permission from Billing and Lemmerer,[58] RSC.

(E) $CsCuCl_3$ chiral 1D perovskite, reproduced with permission from Cao et al.,[59] ACS.

structure deformation can bring chirality to the overall structure.[69] Early studies dating back to the 1970s showed that Cu^{2+} induced Jahn-Teller distortion in $CsCuCl_3$ and produced 1D chiral helical structures (Figure 2E).[66]

Goldschmidt tolerance factor: a simple way to distinguish between A-site substitution and intercalation, and to measure the degree of deformation in the perovskite crystal structure, is to calculate the Goldschmidt tolerance factor. This method is very simple, requiring only the radii of the three ions to be considered, but its effectiveness has been well demonstrated.[70] The relevant formula is as follows[71]: $\tau = \frac{r_A+r_X}{\sqrt{2}(r_A+r_B)}$, where r_A, r_B, and r_X are the ionic radii at the A, B, and X sites, respectively. The tolerance factor τ can be used to measure whether the three ions can stably form 3D perovskite, and the degree of distortion in the crystal structure of the 3D perovskite. The relationship between the tolerance factor τ and perovskite structure is shown in Table 1 below.

It is worth noting that the Goldschmidt tolerance factor can only be used to measure the stability of the classical ABX_3 3D perovskite crystal structure, and does not apply to 3D perovskites with special crystal structures such as (R/S-PyEA)Pb_2Br_6[55] and (R/S-BPEA)$EA_6Pb_4Cl_{15}$.[56]

Transfer mechanism of chirality from surface ligands

The chiral ligands on the surface of the achiral perovskite can induce the perovskite to exhibit chiral properties. These methods have been widely used in semiconductor nanocrystals (NCs), especially in quantum dot (QD) materials. The chiral surface ligands mentioned in this paper include not only chiral organic molecules (such as MBA,[72] PEA,[73,74] MPEA,[73] NEA,[75] DACH,[76] 2OA,[77] ABA,[78] CYS,[79] and BNP[80]) but also other low-dimensional chiral perovskites. In addition to the intrinsic chirality of the surface ligands, there are two main sources of chirality brought by the surface chiral ligands of perovskite crystals: surface distortion and electronic interaction between chiral ligands and achiral substrates.

Surface distortion: due to incomplete surface bonding, the surface of perovskite crystals has many ionic vacancies and suspended bonds, which can be coordinated with chiral ligands (mainly organic amines). These ligands, in turn, distort the inorganic skeleton on the surface of the perovskite crystal, resulting in obvious symmetry breaking and thus obvious chirality. Kim et al. found that this lattice distortion can deeply affect the lattice at depths of up to five monolayers (MLs) (Figure 3A).[72] This chiral introduction is mostly seen in 3D perovskites, but Cao et al. show that it can also be used in 2D/quasi-2D perovskites (Figure 3B). They found that 2D/quasi-2D $CsPbBr_3$ nanosheets modified with chiral ligands (R)/(S)-β-methylphenethylamine exhibit significant optical chirality.[81] In most cases, the chiral ligand ions used in relevant studies are mostly organic cations, but there are also studies using anions as ligands. Tran et al.[80] reported a chiral perovskite using the chiral anion R/S-BNP as a chiral ligand and $CsPbBr_3$ as an achiral base. The optical chirality of R/S-BNP-$CsPbBr_3$ remains unchanged after purification with

Please cite this article in press as: Feng et al., Chiral perovskites: From chirality mechanisms to photovoltaics, Matter (2026), https://doi.org/10.1016/j.matt.2026.102758

Table 1. Relationship between tolerance factor τ and perovskite structure[7,70]

Range of τ	$\tau < 0.77$	$0.77 \leq \tau < 1$	$\tau = 1$	$1 < \tau \leq 1.05$	$\tau > 1.05$
A-site ion	too small	smaller	moderate	larger	too large
Is it perovskite?	no	yes	yes	yes	yes
mechanism of Chirality	–	A-site substitution	A-site substitution	A-site substitution	A-site Intercalation
Characteristics of perovskite structure	–	smaller A-site ions cause the octahedron to tilt and deform, resulting in crystal structure distortion	perfect and ideal perovskite crystal structure with almost no distortion inside the crystal	larger A-site ions prevent the formation of 3D perovskite, but the 3D perovskite can still be relatively stable	too large A-site ions destroy the crystal structure of 3D perovskite and produce low-dimensional perovskite
Dimension	–	3D	3D	3D	2D/1D/0D

antisolvent, owing to the high binding affinity of the phosphate group to the surface of $CsPbBr_3$ perovskite NCs.

Electronic interaction: in addition to surface lattice distortion, electronic interactions between chiral ligands and achiral perovskites are also important mechanisms of chirality in perovskites. Forde et al.[76] used density functional theory calculations to explore the mechanism of chiral transfer in chiral diamino-cyclohexane (DACH) enantiomer-terminated CsPbX3 (X = Cl, I) clusters, and found that the mechanism is more likely to be chiral molecular dipole-cluster transition dipole coupling rather than lattice distortion (Figure 3C). In recent years, CISS has attracted much attention as a novel electron interaction, and related research has focused on NCs and 2D/3D perovskite structures. The former studies have found that chiral perovskite NCs modified by chiral ligands are a good platform for CISS research[75]; the latter studies have found that low-dimensional chiral perovskites can also be regarded as a chiral ligand that can transfer chirality to achiral 3D perovskites through CISS, which is commonly seen in the field of QDs.[82,83]

It is worth mentioning that the chiral ligands filling the ion vacancies on the surface of perovskite not only give the chirality in perovskites but also passivate the surface of perovskite, which has special significance for improving the photoelectron yield of perovskite materials. At present, relevant studies[84] have proved that using ligands with specific chiral structures to passivate perovskite materials has a better effect than using its enantiomers, which provides a new research direction for the application of chiral perovskites in the photovoltaic field. This is explained in detail in the section "application of chiral perovskite in photovoltaics."

Chiral nanostructures beyond the crystal level

The introduction of chirality in perovskites is not necessarily limited to the internal structure of the crystal. Chiral nanostructure designs beyond the crystal level have also been shown to confer chirality on achiral perovskites. Perovskite materials used in such designs generally do not have intrinsic chirality, and their chirality comes from chiral geometric structures beyond the crystal level, with scales generally ranging from a few nanometers to a few millimeters. According to the size of the geometric scale of perovskite, perovskite chiral nanostructures can be divided into two categories: NC assembly and metamaterials.

Perovskite NC assembly: NCs refers to crystalline materials that are only a few nanometers in size, including recently popular QD materials. Chiral assembly of achiral perovskite NCs using chiral gels, polymers, helical SiO_2, and liquid crystals (LC) is a widely used method. In 2018, Shi et al.[85] reported their discovery of the chiral organic lipid N,N′-bis(octadecyl)-L/D-glutamic (abbreviated L/D-Gam) mixing diamide with achiral inorganic perovskite NCs stabilized by oleic acid and oleyl amine forms a co-gel with circularly polarized light emission (CPLE) in a non-polar solvent (Figure 4A). Later, Cao et al.[90] conducted a similar study. They designed and synthesized a simple amphiphilic molecule (D/L-MA-ALA-COOH) that can self-assemble into a chiral gel with helical chirality in a non-polar solvent. The gel is co-assembled with $CsPbX_3$ (X = Cl or Br) NCs to achieve circularly polarized emission of g_{lum} up to 8.2×10^{-3}. In addition, achiral perovskite QDs can theoretically be assembled into chiral QD molecules, as demonstrated by calculations by Tepliakov et al. (Figure 4B).[86]

Perovskite chiral metamaterials: the geometric scale of metamaterials is significantly larger than that of NCs, generally in the tens of nanometers to a few millimeters. According to the way of obtaining the chiral geometry, the synthesis strategies of perovskite chiral metamaterials can be divided into two categories[91]: bottom-up[92,93] and top-down.

The "bottom-up" process relies on a pre-processed base or pre-patterned template and is an accumulation or addition process. The chiral geometry is completed before perovskite synthesis. For example, it is a typical "bottom-up" process to grow achiral perovskites in pre-prepared nano-templates with chiral micro-nano structures to obtain chiral superstructures. Choi et al.[87] prepared different scale nano-templates composed of cholesteric polymer networks to introduce chirality into non-chiral hybrid organic-inorganic perovskite (BZA_2PbI_4, BZA = benzylamine), and observed significant CPLE and circular dichroism (CD) (Figure 4C).

"Top-down" refers to the process of achieving a chiral superstructure after perovskite synthesis. Ion beam/electron beam/laser engraving and nanoimprinting are "top-down" methods that have been used for perovskite metamaterials. Long et al.[88] and Mendoza-Carreno et al.[89] prepared clear gammadion chiral patterns on perovskite surfaces by focused ion beam (FIB) milling and nanoimprinting, respectively (Figures 4D and 4E). Experiments and simulations show that the chiral meta-surface has

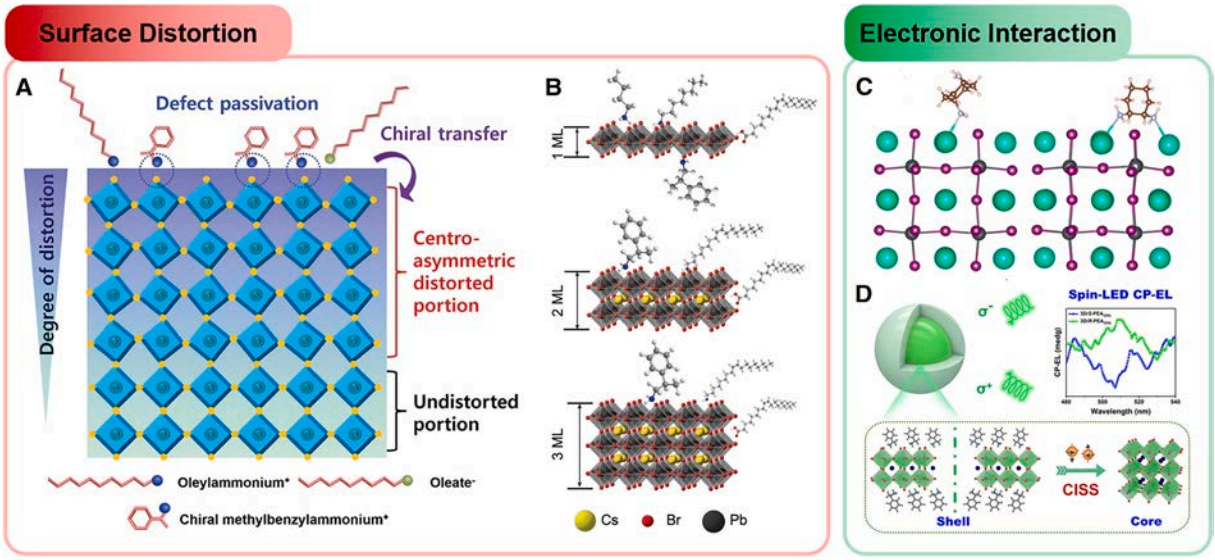

Figure 3. Schematic diagram of transfer mechanisms of chirality between ligand and perovskite

(A) Chirality of 3D perovskites induced by ligands, reproduced from Kim et al.,[72] Wiley-VCH, licensed under CC BY 4.0.

(B) Chirality of 2D/quasi-2D perovskites induced by ligands, reproduced with permission from Cao et al.,[81] Wiley-VCH.

(C) Ligand DACHs bind to a cluster surface in the (left) monodentate and (right) bridging configurations, reproduced with permission from Forde et al.,[76] ACS.

(D) The chiral shell induces the achiral nucleus to exhibit chirality by CISS in the core-shell structure, reproduced with permission from Ye et al.,[82] ACS.

significant chiroptical activity, which provides a new possibility for the detection and emission of circularly polarized light.

In general, because the structure is too macro, there are few studies on the impact of chiral nanostructures on photovoltaic effects. However, studies have shown that metamaterials can reproduce atomic-scale phenomena on a macroscopic scale and use them to achieve molecular-scale functions, which provide a new possibility for using meta-structures to achieve photovoltaic effects, which will be described in detail in the next section.

Novel/multiple mechanisms of chirality in perovskites

It should be emphasized that the chiral crystal structure does not require the ion/ligand to be inherently chiral, such as the B-site ion with Jahn-Teller distortion mentioned above and Sohncke space group caused by A-site achiral ions.[11,94]

In addition to the chirality mechanisms in perovskites mentioned above, novel mechanisms have been emerging in research, such as the chiral crystallization of perovskites induced by nanometer/micron nuclei proposed by Chen et al. being one.[95] The study found that in MABr-$PbBr_2$-DMF (MA = methylammonium, DMF = N,N-dimethylformamide) solution, with carbon, copper, In_2O_3, and other NCs or micron crystals as condensation nuclei, it is possible to grow $MAPbBr_3$ NCs with a chiral crystal structure, even if normal $MAPbBr_3$ is not chiral. This kind of chiral perovskite preparation technology cannot be classified by traditional methods and is a novel chirality mechanism. Although there is less research on these technologies, novel mechanisms of chirality in perovskites hold promise, and their future development is worth looking forward to.

It is worth noting that most types of chirality with distinct mechanisms can coexist within the same perovskite material. It is possible to give a piece of perovskite material multiple mechanisms of chirality. For example, A-site substituted 3D chiral perovskite NCs surface-treated with chiral ligands to give them two types of chirality with distinct mechanisms: in-crystal A-site ions and surface chiral ligands. Or to make chiral nanomaterials from perovskite with molecular chirality as raw materials, such products have two types of chirality at the crystal level and beyond the crystal level. Indeed, the coupling of molecular chirality with metamaterial chirality to achieve enhanced optical chirality has been validated by the study of Zhao et al.,[96] which corroborates the feasibility of multi-chirality coupling in perovskites. On the one hand, perovskite materials with stronger chirality can be obtained by making the signs of different chirality consistent and superimposing them through design. On the other hand, the chirality at different geometric scales enables materials to have optical chirality over a wider spectrum, which provides a new direction for the development of wide-spectrum chiral optics. In addition, multiple mechanisms of chirality may also have potential value in the photovoltaic field, which will be detailed in the section "application of chiral perovskite in photovoltaics."

Having established the conceptual foundations of chiral perovskites, next section now turns to an in-depth assessment of their photovoltaic potential. Chirality introduced via intracrystalline ions enables Rashba splitting and the bulk photovoltaic effect (BPVE)—two distinct mechanisms that respectively offer pathways for improving classical solar cell performance and enabling novel FE-PV devices. Meanwhile, surface chiral ligands impart CISS and defect passivation, which effectively suppress carrier recombination and enhance device efficiency. In addition, these ligands have been shown to improve the mechanical properties of perovskite solar cells, contributing to device durability.

Please cite this article in press as: Feng et al., Chiral perovskites: From chirality mechanisms to photovoltaics, Matter (2026), https://doi.org/10.1016/j.matt.2026.102758

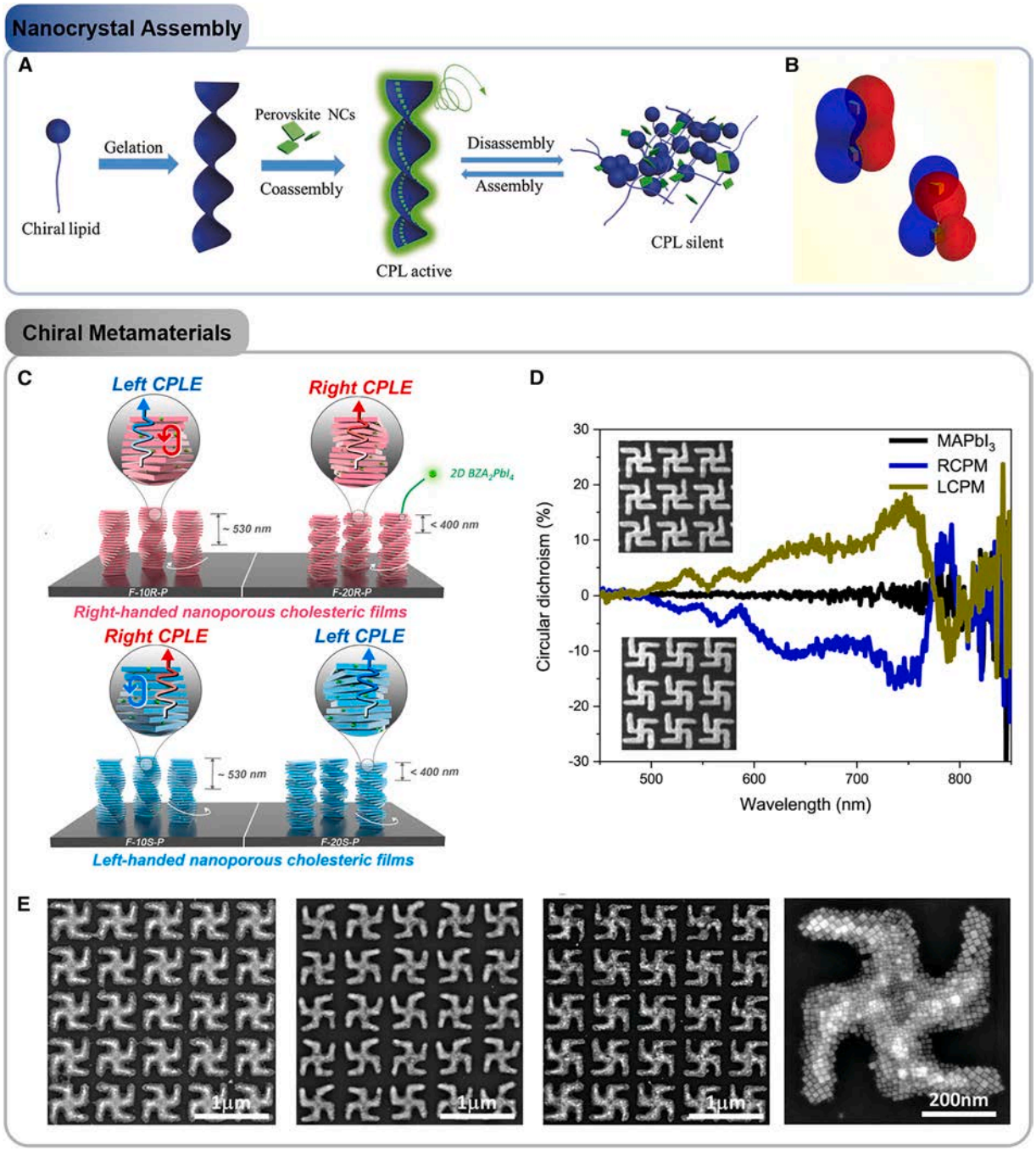

Figure 4. Perovskite chiral nanostructure

(A) Schematic diagram of achiral perovskite NCs co-assembled with chiral gels, reproduced with permission from Shi et al.,[85] Wiley-VCH.

(B) Schematic diagram of perovskite QDs assembled into chiral quantum-dot molecules, reproduced with permission from Tepliakov et al.,[86] ACS.

(C) CPLE difference from nonchiral perovskites incorporated into different nanoporous cholesteric polymer templates, reproduced with permission from Choi et al.,[87] ACS.

(D) CD of perovskite chiral meta-surfaces based on FIB milling, reproduced from Long et al.,[88] Springer Nature, licensed under CC BY 4.0. The inset shows the SEM pictures of perovskite chiral meta-surfaces.

(E) The SEM pictures of perovskite chiral meta-surface based on nanoimprinting, reproduced from Mendoza-Carreño et al.,[89] Wiley-VCH, licensed under CC BY 4.0.

Please cite this article in press as: Feng et al., Chiral perovskites: From chirality mechanisms to photovoltaics, Matter (2026), https://doi.org/10.1016/j.matt.2026.102758

The following section provides a detailed elaboration of these mechanisms and explores the broader prospects and practical feasibility of chiral perovskites in photovoltaic applications.

APPLICATION OF CHIRAL PEROVSKITE IN PHOTOVOLTAICS

Since the first perovskite photovoltaic cell came out in 2009, researchers around the world have fully realized the value of perovskite materials with a large absorption coefficient, high carrier mobility, long carrier life, adjustable band gap, and other characteristics relevant to the photovoltaic field, and started a series of profound and extensive perovskite photovoltaic cell research. Through that research, the energy conversion efficiency has been successfully increased from the initial 3.8% to the most recent 27.3%.[38] However, the research on chiral perovskites in the photovoltaic field is still in its infancy.[97] This section will summarize and expand on current research on chiral perovskites in the photovoltaic field from the perspectives of optimizing classical photovoltaic devices and of developing new photovoltaic devices using various characteristics of chiral perovskites.

Chiral perovskites improving the performance of classical photovoltaics

When a semiconductor absorbs photons that have energy higher than the intrinsic bandgap energy, electrons at the top of the valence band will be excited to transition to the conduction band, producing electrons and holes. In general, these excited carriers decay quickly to the ground state and maintain energy conservation by emitting photons or phonons. However, when the electrostatic potential in a semiconductor has an asymmetric structure (built-in electric field), the recombination of electrons and holes will be affected and move in the opposite direction, resulting in a photogenerated net electron flow and a hole flow, that is, a photocurrent. In addition to adjusting the band gap to absorb a wider spectrum of photons, reducing photovoltaic material defects, inhibiting carrier recombination, and extending carrier lifetimes are also considered important methods to optimize the performance of classical photovoltaic devices. So far, studies have shown that various properties of chiral perovskite materials (the Rashba effect, chiral-induced spin selectivity, etc.) can play a significant role in these aspects.

Rashba effect: Rashba et al.[98] first discovered the Rashba effect in 1959 when studying the band structure of type II wurtzite crystals; it refers to the band splitting caused by spin-orbit coupling (SOC) in a system with single axis symmetry breaking, in which electrons with different spin directions have different band energies. Researchers generally use Rashba parameters or Rashba splitting energy to measure the strength of the Rashba effect. Their relationship is as follows[99]: $2E_R = \alpha_R k_0$, where α_R, E_R (sometimes represented by E_0[100]), and k_0, respectively, refer to the Rashba parameter, the energy difference between the vertex of the energy curve before and after the energy band splitting (i.e., Rashba splitting energy), and the offset of the vertex on the k axis. The definitions of the three are shown in Figure 5A. In addition, the Rashba parameter is sometimes defined as: $\alpha_R = \frac{\Delta E}{2k_0}$, where ΔE refers to the energy difference between the two branches at the vertex of the curve after the band splitting.[104,105] If the energy curve is approximated as a quadratic function curve, it is easy to find that ΔE_R is four times E_0, and the two equations are essentially equivalent. It is worth noting that some papers[106] also refer to ΔE as Rashba splitting energy, which needs to be carefully identified.

For a long time, research on the Rashba effect had been concentrated in the field of spin photonics until Zheng et al.[101] studied the long carrier lifetime of perovskite solar cells in 2015. Since perovskite materials have been used in photovoltaic devices, their relatively longer carrier lifetime compared to silicon-based photovoltaics has attracted researchers' attention. It was once thought that this extraordinary carrier lifetime was due to the lower defect density in perovskite materials, but Zheng et al. demonstrated that the Rashba effect is the main reason for the long carrier lifetime.

As shown in Figure 5B, the Rashba effect increases the spin devolution of the conduction and valence bands near the bandgap, producing an "inner band" (orange arrow) and an "outer band" (cyan arrow) with opposite spin textures "clockwise" ($\chi = -1$) and "counterclockwise" ($\chi = 1$), respectively. After the electron absorbs the photon, it transitions from the valence band to the conduction band (blue arrow), and the excited electrons on the conduction band $C\chi = 1$ and $C\chi = -1$ will rapidly relax to the minimum value of the band $C\chi = -1$ (red arrow) due to inelastic phonon scattering. Similarly, the hole rapidly relaxes to the maximum value of the $V\chi = 1$ band (red arrow). However, since spin states and wave vectors are opposite, the radiative recombination of $C\chi = -1 \rightarrow V\chi = 1$ is a process prohibited by spin and momentum (light blue arrow). In addition, the minimum and maximum values of the $C\chi = -1$ band are located at different locations in the Brillouin zone, which creates an indirect band gap for recombination, further slowing down the recombination process. The combined effect of the two prolongs the carrier lifetime. In this study, Zheng et al. demonstrated their proposed mechanism using first-principles calculations, and showed that the extension of carrier lifetime is positively correlated with Rashba fission energy.

According to Zheng et al., it is easy to imagine that the performance of perovskite solar cells can be improved by enhancing the Rashba effect of perovskite materials to improve the carrier lifetime. The introduction of chiral symmetry breaking has been proven to be a reliable means to enhance the Rashba effect in many studies. Jana et al.[105] showed that 2D perovskite materials with R-(+)- or S-(−)-1-(1-naphthyl)ethylammonium (abbreviated as R-NPB/S-NPB) as the A-site ion, Pb^{2+} as the B-site ion, and Br^- as the X-site ion exhibit a significant Rashba effect and obvious optical chirality. Rac-NPB does not have these characteristics. Li et al.[106] further studied the synthesis of chiral 2D/3D composite perovskite films by mixing chiral organic cations with cesium bromide, and realized a strong Rashba effect by symmetry breaking between chiral and achiral interfaces. To summarize, the performance of photovoltaic devices can be effectively improved by introducing chirality to enhance the Rashba effect, which inhibits carrier recombination, extending the carrier lifetime.

CISS: CISS refers to the phenomenon wherein electrons can be selectively transported or filtered according to the spin state

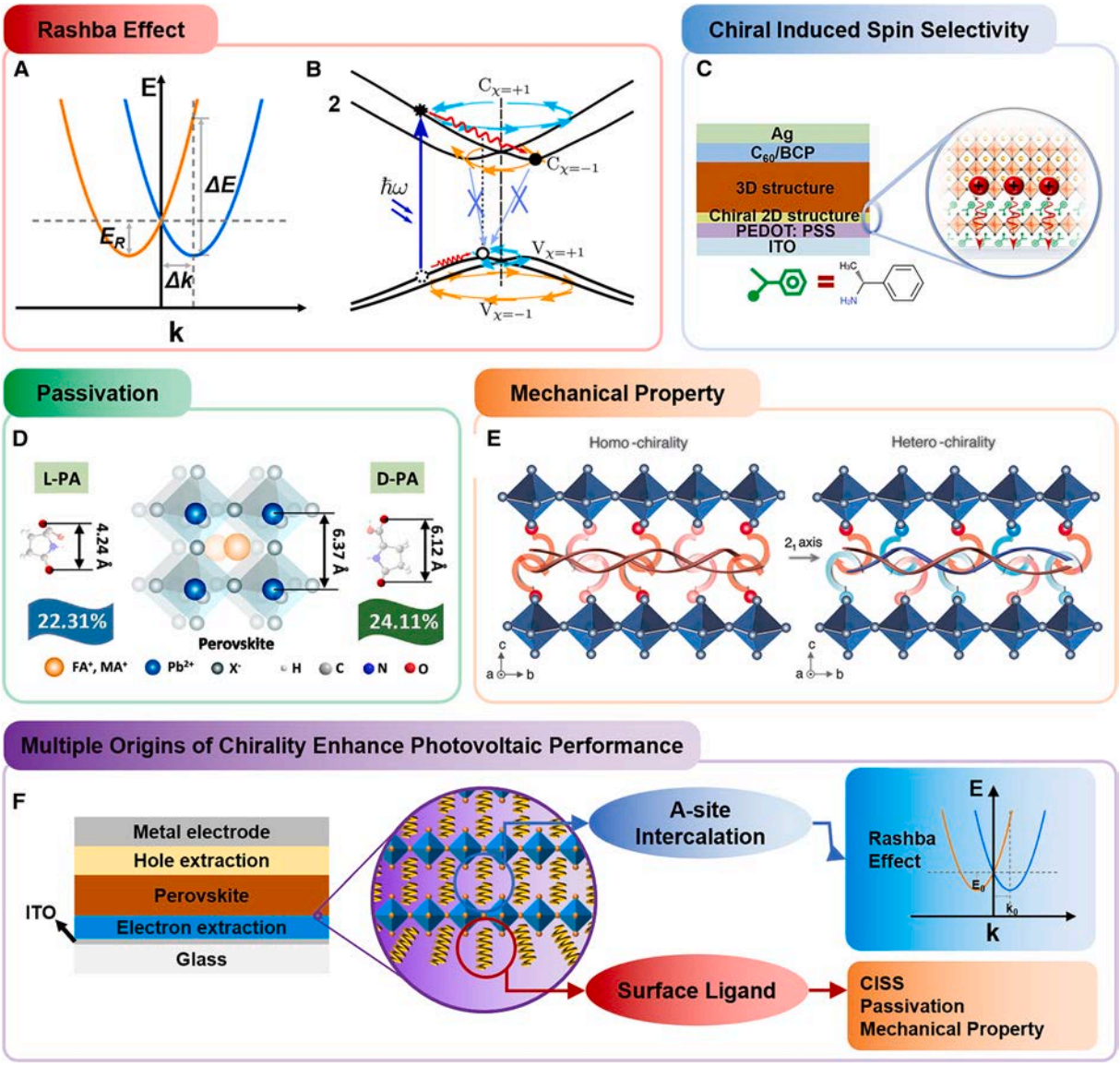

Figure 5. Improvement of traditional photovoltaic performance by chiral perovskite

(A) Illustration of the Rashba effect and related parameters at the bottom of the conduction band.

(B) Diagram of Rashba bands and the electron transport path, reproduced with permission from Zheng et al.,[101] ACS.

(C) Diagram of CISS in chiral 2D/achiral 3D perovskite structures in perovskite solar cells, reproduced with permission from Gao et al.,[102] Elsevier.

(D) The structures and size comparison of passivating agent L/D-pyroglutamic acid (L/D-PA) and $FAPbX_3$, reproduced with permission from Wu et al.,[84] ACS.

(E) Diagram of perovskite solar cells with homo/hetero-chiral interlayers, reproduced with permission from Duan et al.,[103] AAAS.

(F) Schematic diagram of enhancing photovoltaic performance with multiple mechanisms of chirality.

of electrons in a chiral system, which reflects the connection between chiral symmetry and electron spin, and is generally represented by electron transport and electron displacement current. The relevant research can be traced back to the asymmetric scattering of spin-polarized electrons from chiral molecular gases by Lee and Yang shortly after the discovery of parity destruction (i.e., weak force destruction of parity conservation).[107] However, the asymmetry measured in the gas phase was too weak ($<10^{-4}$) until Ray et al.[108] found in 1999 that the scattering asymmetry becomes significant (0.1–0.2) when electrons travel through an ordered film of chiral molecules. With the progress of spin-related studies, the spin asymmetry has been raised to 0.6.[109] As of 2012, this phenomenon is known as CISS.[110]

Unfortunately, the principle of CISS is not fully understood, but it is generally believed to be closely related to SOC, similar to the Rashba effect.[111] Moreover, CISS has also been found to effectively optimize the performance of photovoltaic devices. Gao et al.[102] showed that chiral perovskites can promote hole transport in perovskite solar cells. As shown in Figure 5C, they added

Please cite this article in press as: Feng et al., Chiral perovskites: From chirality mechanisms to photovoltaics, Matter (2026), https://doi.org/10.1016/j.matt.2026.102758

a layer of MBAI to the $FASnI_3$ perovskite solar cell and obtained a 2D/3D thin film structure (mechanism II of chirality). Using a magnetic conductivity probe atomic force microscope (mCP-AFM) to investigate the charge transport effect of the chiral thin film, they found that $(R\text{-}/S\text{-}MBA)_2SnI_4$, formed after the addition of the R-/S-MBA layer to the $FASnI_3$ solar cell, exhibited a CISS induced charge transport effect. CISS is beneficial to the interface extraction of positively polarized charge, and the rapid charge transfer and efficient hole transport it enables further reduce the interface charge recombination and inhibit the hysteresis effect in PSC devices. The $(rac\text{-}MBA)_2SnI_4$ did not show CISS, although rac-MBA based devices did show better photovoltaic performance than non-MBA devices, but only because the PEDOT:PSS/$FASnI_3$ interface has better level alignment (i.e., passivation effect) under the influence of 2D MBA_2SnI_4; the performance of rac-MBA devices is not as good as that of R/S-MBA devices with CISS. Although the mechanism of CISS is not yet fully studied, this study fully demonstrates the potential of CISS to optimize photovoltaic devices by improving interfacial charge extraction. However, this study only validated the optimization of interface extraction for positive charges. Although the interface extraction of negative charge could also be improved by CISS, the specific experimental verification still needs further research work.

Passivation: In addition to the above-mentioned, chiral perovskites have also been found to optimize photovoltaic devices in other ways. As we all know, the passivation of photovoltaic materials is one of the important methods to optimize the performance of photovoltaic devices; it can reduce carrier recombination due to defects in or on the surface of the materials and extend the life of perovskite solar cells.[112–117] The chirality of the passivating agent has been found to have a significant impact on the passivating effect: some chiral molecular structures match the A-site ion defects of perovskites better than their enantiomers. Wu et al.[84] found that when the chiral molecules L- and D-pyroglutamic acid (L-PA and D-PA) were used as additives for perovskite passivation, both of them significantly improved the photovoltaic performance of the materials, but the effect of the latter was significantly better than that of the former. This is because L-PA has a more twisted spatial configuration, while D-PA is more planar, resulting in a difference in distance between the two C=O groups. As shown in Figure 5D, the smaller distance between the two C=O groups of L-PA compared to the Pb–Pb bond length will distort the perovskite lattice structure, resulting in poor device stability. In contrast, the similar distance between the two C=O groups of D-PA with the Pb–Pb bond length promotes the preferentially oriented growth of perovskites. In addition, it has been found that the chiral environment of L-cys shows advantages in terms of inhibition of non-radiative recombination, perovskite crystallization, stability, and light capture.[79] Between the two, L-cys is superior to D-cys due to the difference in their electrostatic potential distributions, which makes their abilities to bind with perovskite defects different, resulting in different passivating abilities.

Mechanical properties: In addition to passivation, the improvement of mechanical properties of solar cells by chiral structures has recently received attention.[118,119] Duan et al.[103] published a study in *Science* showing that using R-/S-/rac-MBAI as the intermediate layer of organic-inorganic hybrid perovskite solar cells can not only effectively passivate perovskite materials and reduce carrier recombination, but also significantly improve the mechanical properties of the cells and enhance delamination resistance and toughness. In the study, the mechanical properties of the heterogeneous chiral perovskite interface (rac-MBAI intermediate layer) are superior to those of the homogeneous chiral perovskite interface (R-/S-MBAI intermediate layer). The latter acts like a molecular spring, enhancing the elasticity of the interface, but is more prone to elastic deformation, resulting in a small Young's modulus, as shown in Figure 5E. In contrast, heterochiral perovskite interfaces formed between enantiomers with opposite chirality exhibit a greater Young's modulus while maintaining excellent elastic recovery. Therefore, although both homogeneous and heterogeneous chiral perovskite interfaces show improved mechanical properties, heterogeneous chiral perovskite interfaces reduce elastic deformation under the same stress and have better mechanical properties. This study provides a new direction for research in photovoltaics. Previously, most researchers have focused on the photoelectric conversion performance and temporal stability of photovoltaic devices, but this study may inspire researchers to optimize other aspects of photovoltaic device performance, such as mechanical stability and resistance to extreme temperatures.

Idea (I) multiple mechanisms of chirality enhancing photovoltaic performance: The previous section mentioned that the multiple mechanisms of chirality can effectively enhance the optical chirality intensity and spectrum width of perovskite materials. Combined with the content of this section, it can be inferred that multiple mechanisms of chirality also have great potential to improve the performance of perovskite solar cells. For example, Rashba effects are often seen in 2D chiral perovskites based on A-site intercalation (mechanism I of chirality), while CISS is more often seen in chiral perovskites with surface chiral ligands (mechanism II of chirality). It is easy to think that if a chiral perovskite has two chirality mechanisms, from A-site intercalation and surface chiral ligands, then it may have a long carrier lifetime from the Rashba effect and a strong charge extraction ability from CISS, and thus have a stronger photovoltaic performance. Similarly, passivation and mechanical properties improvements are also based on surface chiral ligands, and chiral perovskites with both A-site intercalation and surface chiral ligands may have the effects of long carrier lifetimes from the Rashba effect, and improved passivation/mechanical properties at the same time (Figure 5F). It is acknowledged that leveraging multi-chirality coupling for photovoltaic enhancement is still an unverified idea. Nevertheless, its effectiveness in boosting chiral optical responses has been substantiated by existing research,[96] thereby reinforcing the prospects for its extension to photovoltaics.

Chiral perovskites facilitating the development of novel photovoltaics

As mentioned above, the photovoltaic effect relies on a built-in electric field to separate the two kinds of carriers, electrons and holes. In general, the built-in electric field in photovoltaic devices is derived from the PN junction (a heterogeneous structure composed of P-type semiconductors and N-type semiconductors). The power generation performance of such photovoltaic

Please cite this article in press as: Feng et al., Chiral perovskites: From chirality mechanisms to photovoltaics, Matter (2026), https://doi.org/10.1016/j.matt.2026.102758

Table 2. Examples of chiral perovskite ferroelectrics

A-site chiral molecule (abbreviation)	Chemical formula	Dim	Reference
R/S/rac-3-ammoniopyrrolidinium (R/S/rac-3AP) R/S/rac-3-ammonioquinuclidinium (R/S/rac-3AQ)	R/S/rac-3AP–NH_4X_3 R/S/rac-3AQ–NH_4X_3 (X = Cl or Br)	3D	Ye et al.[54]
R/S-3-fluoropyrrolidinium	R/S-3-(fluoropyrrolidinium)MnX_3 (X = Cl or Br)	1D	Ai et al.,[45]; Gao et al.[120]
R/S-1-(4-chlorophenyl) ethylammonium	[R/S-1-(4-chlorophenyl)ethylammonium]$_2PbI_4$	2D	Yang et al.[44]
(R)/(S)-(−)/(+)-1-cyclohexylethylamine (R/S-CYHEA)	(R/S-CYHEA)PbI_3	1D	Hu et al.[121]
(R)-(−)-1-methyl-3-phenylpropylamine (R-MPA)	(R-MPA)$_2CdCl_4$	0D	Li et al.[122]
2,2′-dithiobis(ethylamine) dihydrochloride[a] (Cystamine, Cysta)	CystaH_2CuCl_4	2D	Deng et al.[65]
(R)-N-ethyl-3- quinuclidinol (R-EQ)	(R-EQ)PbI_3	1D	Fu et al.[123]
(R)/(S)-N-(1-phenylethyl)ethane-1,2-diaminium (R/S-PEDA)	(R/S-PEDA)PbI_4	2D	Zeng et al.[124]
(R)/(S)-3-F-pyrrolidinium	(R)/(S)-3-F-(pyrrolidinium)$CdCl_3$	1D	Tang et al.[46]
(R)/(S)-3-(aminomethyl)-piperidine (R/S-3AMP)	(R/S-3AMP)$PbBr_4$	2D	Fan et al.[125]
4-phenylbutylamine[b] (4PBA)	4PBA-$CdCl_4$	2D	Li et al.[126]

[a]2,2′-Dithiobis(ethylamine) dihydrochloride is not intrinsically chiral, but it can be twisted into a chiral helical structure under the influence of an external electric field in CystaH_2CuCl_4.
[b]4-Phenylbutylamine is also not intrinsically chiral, but its induced lattice distortion and its own distortion together constitute a chiral structure.

devices will also be restricted by the performance of the PN junction. The performance of the PN junction is limited by semiconductor materials. In theory, photovoltaic devices based on PN junctions have an upper conversion limit, the Shockley-Queisser limit, due to the limited band gap width of the semiconductor materials. However, some photovoltaic effects do not depend on the PN junction structure and are not limited by the Shockley-Queisser limit, known as anomalous photovoltaic (APV) effects. Among them, the FE-PV effect is one of the most common anomalous effects and has attracted much attention.

The property of ferroelectrics to generate photovoltage and photocurrent under uniform light is called the FE-PV effect. Because the asymmetry of chiral perovskites can effectively induce the generation and spontaneous polarization of electric dipoles, it can be inferred that chiral perovskites have great potential in the field of ferroelectrics, which is proven by relevant studies (Table 2). Additionally, the potential of perovskite materials for photovoltaic applications has been fully demonstrated. Considering both of these points, the potential value of perovskite for FE-PVs can be inferred.

As an APV effect, the FE-PV effect can exceed the band gap limit of photovoltaic materials without a PN junction, and can also change the direction of spontaneous polarization by electric field to switch the direction of current. Therefore, the FE-PV effect is considered to have great potential for the development of new photovoltaic devices. However, the mechanism of the FE-PV effect is complex and not unique, and in ferroelectric materials, photogenerated charge carriers can be separated by multiple forces. At present, the main sources of the FE-PV effect include the BPVE, ferroelectric domain wall theory, depolarization field, Schottky junction, and so on. For a detailed analysis, this section will discuss the mechanism of the FE-PV effect, and then explore the potential and value of chiral perovskites in this context.

BPVE in chiral perovskites: The BPVE, sometimes called the photogalvanic effect (PGE), refers to the characteristics of homogeneous materials under uniform light irradiation to produce current, and the biggest difference compared with the classical photovoltaic effect is that there is no heterostructure. BPVEs have been found mainly in ferroelectrics, first in $BaTiO_3$ in the 1970s. Historically, the built-in electric field formed by macroscopic polarization in materials has been considered to be the origin of the BPVE, which is also the most popular and simplest intuitive explanation of the FE-PV effect. However, with the progress of related research, more theoretical models have been proposed (Figure 6)[127,133]: (i) some early models believe that the asymmetric scattering center with the same orientation in the materials is the source of the photocurrent (Figure 6A)[128]; (ii) other theories hold that the asymmetry of the electrostatic barrier makes carriers with energy in a specific range only move in a limited direction, resulting in the generation of photocurrent (Figure 6B)[129]; (iii) some other theories hold that the transition

Please cite this article in press as: Feng et al., Chiral perovskites: From chirality mechanisms to photovoltaics, Matter (2026), https://doi.org/10.1016/j.matt.2026.102758

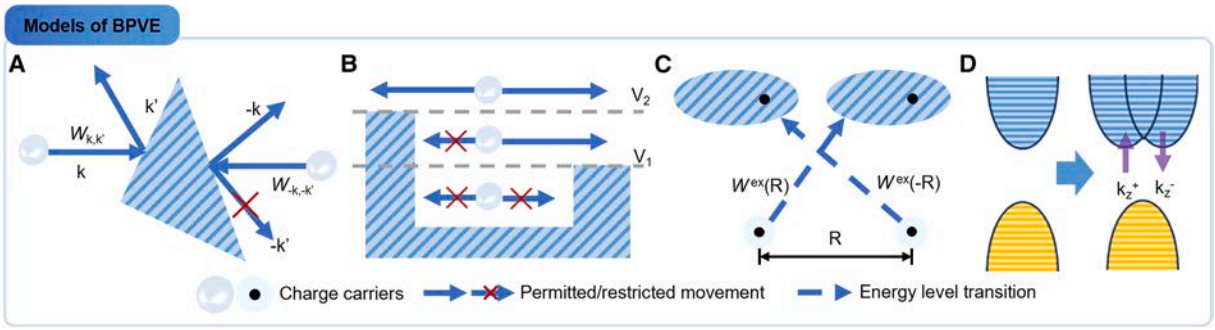

Figure 6. Several models of the BPVE

(A) Asymmetric carrier scattering center, where ±*k* refers to the carrier momentum before scattering, ±*k*' refers to the symmetric carrier momentum after scattering, $W_{k,k'}$ and $W_{-k,-k'}$ refers to the probability of *k*→*k*' and −*k*→−*k*', respectively. $W_{k,k'} > W_{-k,-k'}$, the carrier direction after scattering is asymmetrical.[127,128]

(B) Asymmetric potential well at carrier generation, where carriers with energies between V_1 and V_2 have asymmetric velocity distributions due to the higher potential barrier on the left.[129]

(C) The hopping of a photoexcited electron between two identical centers located at a distance R can also produce a photocurrent in a non-centrosymmetric medium, where $W^{ex}(\pm R)$ refers to the probability of excitation of the electron with a transition. Due to the wave function of the excited state being distorted compared with that of the localized ground state, $W^{ex}(R) > W^{ex}(-R)$ and the carrier momentum distribution is asymmetrical.[130,131]

(D) Relativistic splitting of the conduction band minimum establishes two distinct channels (k_z^+ and k_z^-) for electron excitation, polarized light promotes electrons preferentially to one channel.[132]

asymmetry caused by the distortion of the excited state wave function is the cause of the net photocurrent generation (Figure 6C)[130,131]; (iv) still other theories have found that the Rashba effect, caused by the strong SOC, can explain the BPVE under polarized light (Figure 6D).[132] Now, models based on time-dependent perturbation theory have become the mainstream explanation of BPVEs.

In the model, the BPVE is considered the result of two currents: the shift current and the ballistic current. The former originates from the off-diagonal part of the electron density matrix and is caused by the carrier shift during the photoinduced transition. The latter is derived from the diagonal portion of the electron density matrix and is caused by the asymmetry of the carrier momentum distribution.[134,135] The two current theories have some similarities with other BPVE models mentioned above: both shift current and model III are related to the asymmetric displacement of carriers during the energy band transition; both the ballistic current and model II are related to the asymmetric momentum (velocity) distribution of carriers in the energy band. In fact, as with the other models, the study of the two currents also dates back to early work in the last century, detailed in Fridkin's review.[130] However, better than other earlier theories, the shift current theory was adapted in 2012 by Young and Rappe and can be calculated based on first principles.[136] Then, a first-principles model of ballistic currents was also reported in 2021.[137,138] These studies have led to better simulation and prediction capabilities for the two current models and have helped them become mainstream models of BPVEs. It is worth mentioning that injection current, as a special ballistic current, generally exists only under circularly polarized light, and has a wide range of applications in experiments.

The research and development of the BPVE has been closely related to perovskite materials, from the initial BaTiO3 to the present organic and inorganic hybrid perovskite materials. Incidentally, compounds with chiral structures are thought to have the potential to generate strong displacement currents.[130] Therefore, chiral perovskites are highly relevant in the field of BPVEs. In fact, researchers did find BPVEs in many chiral perovskites, as shown in Table 3 below.

In summary, it can be confirmed that the BPVE exists widely in chiral perovskites. However, there is no consensus on the role of chirality in the BPVE of perovskite. Huang et al.'s study suggests that polarity rather than chirality is the main cause of the BPVE.[143] However, another study showed that the key to the BPVE is symmetry breaking, and the polarity is primarily for enhancing the photocurrent.[139] Although controversy still exists, considering that the BPVE found so far mainly appears in inversion symmetry-breaking materials, there is reason to believe that chiral perovskites with significant symmetry breaking have the potential in the bulk photovoltaic field. The value of chirality and what role it can play in bulk photovoltaics needs further research.

Ferroelectric domain walls based on chiral perovskites: spontaneous polarization of the electric dipole moment is an inherent property of ferroelectrics. When a ferroelectric is spontaneously polarized, the energy increases, the state is unstable, and the crystal tends to be divided into many parts. The electric dipoles within a given part are polarized in the same direction, and the electric dipoles in different parts are polarized in different directions. These parts are called electric domains, and the boundary between electric domains is called a domain wall (Figure 7A). Some studies have shown that the FE-PV effect is related to the domain wall. A study in 2002 found electrostatic dipole moments on both sides of a 90° domain wall (Figure 7B), which lead to electrostatic potential steps as well as valence and conduction band shifts.[146] A study in 2010 found that the FE-PV effect voltage perpendicular to the domain wall is significantly stronger than the voltage parallel to the domain wall, and is positively correlated with the number of domain walls and electrode distance (Figure 7C).[147] To explain this phenomenon, a

Table 3. Some chiral perovskites with bulk photovoltaic effects

A-site chiral molecule (abbreviations)	Chemical formula	Dim	Reference
(R)-(−)-1- cyclohexylethylamine (R-CYHEA)	$(R\text{-}CYHEA)_8Pb_3I_{14}$	1D	Noma et al.[139]
(R)/(S)-β- methylphenethylammonium (R/S-MPA)	$(R/S\text{-}MPA)_2(MA)Pb_2I_7$ (MA = methylammonium)	2D	Huang et al.[140]
(R/S)-1-(4-bromophenyl)- ethylammonium (R/S-BEPA)	$(R/S\text{-}BEPA)_2(FA)Pb_2I_7$ (FA = formidinum)	2D	Ye et al.[141]
R/S-1-phenylpropylamine (R/S-PPA)	$(R/S\text{-}PPA)_2BiI_5$	0D	You et al.[142]
(R)/(S)-β-methylphenethylammonium (R/S-MPA)	$(R/S\text{-}MPA)_2PbI_4$	2D	Huang et al.[143]
(R)/(S)-β-methylphenethylammonium (R/S-MPA)	$[(R)/(S)\text{-}MPA]_4AgBiI_8$	2D	Li et al.[144]
R/S-1-(1-naphthyl)ethylamine (R/S-NEA)	$(R/S\text{-}NEA)[PbI_3]$	1D	Ishii et al.[145]

ferroelectric domain wall photovoltaic theory has been proposed. Ferroelectric domain walls have a built-in potential step generated by the polarization component perpendicular to the domain wall,[146,149] and an electric field is generated between the domains, that is, within the domain wall, which can separate the charge carriers and is perpendicular to the domain wall. The photoexcited electrons and hole pairs separate and drift to both sides of the domain wall, allowing the accumulation of different charges to produce a BPVE, similar to the classical PN junction. It is worth mentioning that each domain wall under this theory can be regarded as a voltage source on the micron/nanometer scale. Most ferroelectrics have more than one domain wall, and many ferroelectric domain walls are connected end-to-end along the polarization direction of the ferroelectric materials, just as many voltage sources are in series. From this, unusually high voltages that are not limited by the band gap of ferroelectric materials can be observed. In addition, because the direction of polarization and the domain walls are affected by the external electric field, the direction of the domain walls can be changed by applying an external electric field, changing the direction of the photocurrent from the FE-PV effect.

Considering that the spontaneous polarization of electric dipoles in ferroelectrics comes from the asymmetry of the crystal structure, and the electric field of ferroelectric domain walls comes from the difference in polarization direction on either side of the domain wall, it can be reasonably inferred that chiral perovskites with obvious asymmetric crystal structures should have obvious influence on the FE-PV effect. Unfortunately, that idea has not been supported by reliable research. However, by review of previous studies, we propose that it may be possible to realize artificial ferroelectric domain walls through chiral perovskites to achieve FE-PV effects.

Concept (I) ferroelectric domain walls based on molecular chirality: the research on the generation of high voltages by ferroelectric domain walls is accompanied by the design and fabrication of artificial ferroelectric domain walls. As early as 2009, Yang et al.[147] achieved the stacking of BiFeO3 thin layers with different electric dipole directions by controlling the annealing process, and realized artificial ferroelectric domain walls that could generate high photogenerated voltages (Figure 7D). Inspired by this, we hypothesized that chiral perovskites could be utilized to achieve a similar effect (Figure 7E). The opposite of perovskite chirality implies a difference in crystal structure and orientation, might meaning different directions of electric dipole moments. If these opposite-handed perovskite thin layers are alternately stacked, it is possible to achieve a new type of artificial ferroelectric domain wall that can generate a high photogenerated voltage (Figure 7E). This design has its unique advantages: on the one hand, there is no need for deliberate annealing control; on the other hand, chiral perovskites are mostly two-dimensional, and due to the presence of the organic spacer layer, it is easier to prepare thin layers. However, the presence of the organic interlayer may also affect the carrier transport. Its superiority still needs to be verified.

Concept (II) ferroelectric domain walls based on chiral metamaterials: the researchers have designed various metamaterial structures to achieve atomic-scale phenomena at the nanoscale,[150–156] including domain walls.[157] A study in 2013 by Kang et al.[148] reported a chiral metamaterial that can switch chirality using a flexible material (Figure 7F). They found that this flexible metamaterial can have different geometric shapes in different parts of the same material, some of which have opposite geometric chirality. They call a part of consistent chirality a domain. Unfortunately, they did not focus on the walls between the different domains. In 2020, Deng et al.[158] conducted a similar study and focused on domain walls, suggesting that they could be designed with different shapes through the mechanical deformation of flexible metamaterials. Inspired by these findings, we hypothesize that the metamaterial domain walls might also be applicable to ferroelectrics, that is, metamaterial ferroelectric domain walls (Figure 7F).

Two design ideas are proposed to make the two sides of the metamaterial domain wall have different polarity. (i) Photoexcited unit cells: through the design of different unit cells on both sides of the domain wall, the unit cells on both sides become electric dipoles in different directions under the excitation of electromagnetic waves (light fields). It is a common phenomenon for dielectric elements to have dipoles or even multipoles when excited by

Please cite this article in press as: Feng et al., Chiral perovskites: From chirality mechanisms to photovoltaics, Matter (2026), https://doi.org/10.1016/j.matt.2026.102758

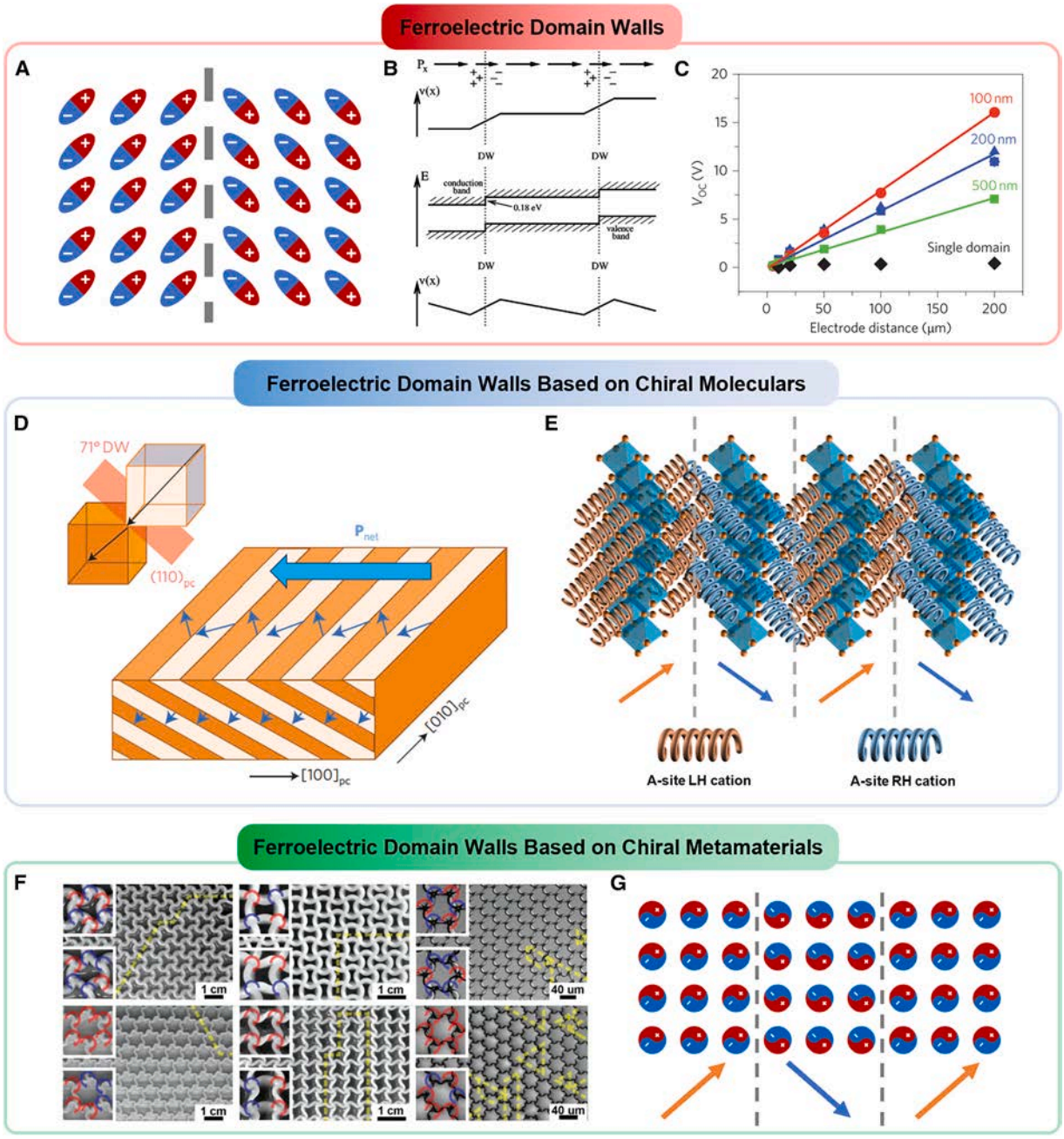

Figure 7. Photovoltaic theory of ferroelectric domain walls and conception of metamaterial ferroelectric domain walls

(A) Schematic of ferroelectric domain walls.

(B) Schematic illustration of a periodic array of 90° domain walls, reproduced with permission from Meyer and Vanderbilt,[146] APS. The upper shows the component P_x of the polarization perpendicular to the DW, and the resulting induced charge and electron potential $v(x)$; the middle shows corresponding band offsets; the lower shows potential $v(x)$ in the case of the corresponding supercell calculation using periodic boundary conditions, i.e., in which the supercell-averaged electric field is zero.

(C) Study of the evolution of V_{OC} as a function of electrode spacing for four different samples: 71° domain-walls samples with thicknesses of 100 nm (red), 200 nm (blue), and 500 nm (green) as well as a monodomain BFO film having no domain walls (black), reproduced with permission from Yang et al.,[147] Springer Nature. A clear correlation between the number of domain walls and the magnitude of V_{OC} is observed.

(D) Schematic diagram of artificial $BiFeO_3$ ferroelectric domain wall, reproduced with permission from Yang et al.,[147] Springer Nature.

(E) The envisioned artificial ferroelectric domain wall based on chiral perovskites.

(F) Domains and domain walls in flexible mechanical metamaterials, where dashed yellow lines represent domain walls, reproduced with permission from Kang et al.,[148] Wiley-VCH. The upper three pictures are achiral, and the lower three pictures are chiral.

(G) Schematic of the hypothesized metamaterial ferroelectric domain wall.

Please cite this article in press as: Feng et al., Chiral perovskites: From chirality mechanisms to photovoltaics, Matter (2026), https://doi.org/10.1016/j.matt.2026.102758

electromagnetic waves.[88] (ii) Ferroelectric unit cells: the use of ferroelectric systems with inherent electric dipole moments can also give the unit cells polarity. In this way, the polarization direction of the two sides of the domain wall is different because of the different unit cell designs on both sides of the domain wall, which puts forward higher requirements for the regulation of the polarization direction. It can be found that the characteristics of chiral perovskite have the potential to make ferroelectric domain walls of metamaterials. Perovskite unit cells can easily become electric dipoles under electromagnetic excitation and be used as optical field excitation unit cells. At the same time, many chiral perovskites are themselves good ferroelectrics and can be used to make ferroelectric unit cells.

The ferroelectric properties (i.e., polarization direction and strength) of metamaterial ferroelectric domains are mainly determined by the microgeometric design of the metamaterials, whether they are photoexcited or ferroelectric unit cells. In addition, photoexcited unit cells are also affected by the dielectric property of the materials itself and the external excitation light field, and ferroelectric unit cells are affected by the ferroelectric property of the materials itself. This makes metamaterial ferroelectric domain walls more stable: the polarization of the photoexcited unit cell depends only on the dielectric property of the materials, the design of the unit cell and the excitation light field. As long as the temperature change does not significantly change the nanostructure of the metamaterial or the dielectric property of the materials, its ferroelectric property will not change obviously (no Curie temperature). For the same reason, ferroelectric domains of metamaterials are not susceptible to ferroelectric fatigue, which provides a new possibility for fatigue-resistant ferroelectrics. However, the relatively large scale of the metamaterial unit cells has inhibited the transfer of charge carriers between the cells, which remains an open question.

Both molecular chirality-based and metamaterial chirality-based artificial ferroelectric domain walls exhibit strong tunability. Owing to the compositional flexibility of perovskites and the design freedom of metamaterial structures, different polarization directions and magnitudes can be achieved by adjusting the type and proportion of chiral molecules/ions or through rational metamaterial design. As demonstrated by Jia et al.,[159] tailoring ferroelectric polarization enables modulation of the interaction between ferroelectric materials and light. This tunability of artificial ferroelectric domain walls suggests the possibility of tailoring the absorption spectrum for FE-PV effects, thereby enabling specific spectral absorption or even broadband absorption to improve power conversion efficiency.

Furthermore, owing to the intrinsic geometrical nature of chirality, artificial domain walls based on chiral perovskites typically also function as crystallographic mirror planes. A study[160] on ferroelastic domain walls suggests that such crystallographic mirror planes can be regarded as defining the orientation of domain walls, and the resultant domains facilitate charge carrier transport, thereby enhancing optoelectronic performance. By analogy, in the context of FE-PVs, artificial ferroelectric domain walls based on chiral perovskites are expected to benefit from improved charge carrier transport, offering a potential pathway toward enhanced photovoltaic performance.

It is worth noting that the ferroelectric domains in achiral perovskites can sometimes exhibit optical chirality,[161–163] but this situation is beyond the scope of discussion in this article.

Depolarization field in chiral perovskites: ferroelectric materials will be polarized under the influence of an external electric field. The microcosmic manifestation of this is that the direction of electric dipoles inside ferroelectric materials tends to be the same. At the same time, due to the influence of the external electric field, a large number of polarized charges appear on the surface of ferroelectric materials. When the external electric field is removed, the polarization remains unchanged, and the materials have a large residual polarization intensity. If the free charge on the electrode surface cannot completely shield the polarized charge, the residual polarized charge will generate an electric field on the ferroelectric materials. This electric field is called the depolarization field. The depolarization field, which exists in the entire ferroelectric material and is similar to the built-in electric field in PN-junction photovoltaic devices, has also been found to separate charge carriers and plays an important role in the FE-PV effect. Relevant studies can be traced back to the study on $BaTiO_3$ in 1956.[164]

Because the depolarized field acts as a carrier separator, the FE-PV effect is positively correlated with the intensity of the depolarized field. Considering that the depolarization field is the electric field generated by polarized charge, according to basic knowledge of electrostatic field distributions, thin materials are more conducive to generating a larger depolarization field, and most studies on the depolarization field also focus on ferroelectric thin films.[165–167] For convenience, thin-film ferroelectrics are illustrated below. The size of the depolarization field E_{dep} can be obtained from the classical electrostatic field within the boundary conditions of the film, as shown in the following equation[168]: $E_{dep} = P/\varepsilon_0\varepsilon_{ferro}$, where P is the average degree of ferroelectric polarization in the film region, and ε_0 and ε_{ferro} are the vacuum and static permittivity of the materials, respectively. The average degree of ferroelectric polarization P is the volume average of the electric dipole moment, calculated by the following formula[169]: $P = \sum P_{dip}/V$, where P_{dip} refers to the electric dipole moment and V refers to the film volume. The depolarization field is positively correlated with the electric dipole moment in the ferroelectric materials.

The electric dipole moment is essentially a symmetry breaking of the charge distribution. In chiral molecules, the charge distribution is usually asymmetric, resulting in an inherent electric dipole moment of the molecule. The electric dipole moment is the result of the misalignment of the positive and negative charge centers in the molecule, which is particularly common in chiral molecules, and the same is true for chiral crystals. It can be inferred that the asymmetric structure of chiral perovskite helps to induce the positive and negative charge centers of the lattice to be non-coincident, resulting in a large number of inherent electric dipole moments with the same direction and size within the materials, which leads to considerable ferroelectric polarization and a significant depolarization field, conducive to the FE-PV effect. The large number of ferroelectrics found in chiral perovskites supports our hypothesis.

In addition to these mentioned above, Schottky junctions have also been found to play an important role in FE-PVs. Although it

Please cite this article in press as: Feng et al., Chiral perovskites: From chirality mechanisms to photovoltaics, Matter (2026), https://doi.org/10.1016/j.matt.2026.102758

has been proven that Schottky junctions play an important role in the FE-PV effect, and it has been found that some Schottky junctions are affected by chiral structures,[170] this paper will not elaborate on them much because Schottky junctions are not intrinsic properties of materials, and no obvious relationship between Schottky junctions and chiral perovskites has been found.

In summary, the application potential of chiral perovskites in photovoltaics is unexpectedly strong. However, there are still some problems in the application of chiral perovskites to PV devices without a PN junction. For example, compared with mature classical photovoltaic devices, the current and conversion efficiency of the FE-PV effect is generally smaller, which may be related to the wide band gap of ferroelectric devices currently used for FE-PVs and weak absorption of low-energy photons. These issues are discussed in the next section.

CHALLENGES AND PROSPECTIVE

There are still many problems and challenges in the application of chiral perovskites in the photovoltaic field, but there is no lack of exciting research directions and bright prospects. In addition to the aforementioned "multiple mechanisms of chirality in perovskites" and "ferroelectric domain walls based on chiral perovskites," this section summarizes the current main research directions and puts forward ideas for possible future research, which are divided into several parts, such as the mechanisms of chirality in perovskites and applications of chiral perovskites.

Challenges and prospects of chirality mechanisms in perovskites

3D chiral perovskite synthesis: considering that 3D perovskite generally has a narrower band gap, higher carrier mobility, and a higher upper limit of photoelectric conversion efficiency than 2D perovskite, the development of 3D chiral perovskite materials has been of interest for a long time. However, in the classical perovskite 3D crystal structure, the A-site ions are confined to the space surrounded by eight regular octahedrons and cannot have a large volume, which restricts further development of chiral 3D perovskites, because the common chiral ions are mostly organic ions with larger volumes. One possible solution is expanding the crystal skeleton to leave more room for the chiral ions, where the research can be summarized in two directions. One of them is to retain the traditional ABX_3 structure while replacing ions other than the A-site with larger ions to expand the volume of the entire cell. Relevant studies have achieved results by replacing the B-site ions with ammonium ions (Figure 2A).[54] The other is to abandon the ABX_3 structure and choose the hetero-skeleton to give the A-site ions more space, and the relevant results are more than the former (Figures 2B and 2C).[55,56] In essence, both methods are expanding the cell skeleton to accommodate larger A-site chiral ions, which is currently the most promising direction of research.

AI-assisted chiral metamaterial design: with the development of artificial intelligence, the use of new technologies, such as neural networks to assist in the development of new materials, especially metamaterials, has gained widespread attention. As early as 2008, genetic algorithms were used to design parameters for a gammadion chiral metamaterial.[171] In recent years, new artificial intelligence methods such as deep learning have been widely used in the chiral metamaterial design of other structures.[172,173] Compared with traditional design methods, using artificial intelligence has the advantages of high speed and low cost while ensuring considerable accuracy. In addition, it is worth mentioning that some studies have found that chiral perovskites can be used to develop photonic artificial synapses to build a neuromorphic vision system,[174] and chiral perovskite materials also show potential in nurturing the development of artificial intelligence technology.

Multiple mechanisms of chirality in perovskites: as noted at the end of the sections "novel/multiple mechanisms of chirality in perovskites" and "chiral perovskites improving the performance of classical photovoltaics," it is theoretically feasible for a single perovskite material to simultaneously exhibit chirality originating from different sources—such as chiral A-site cations within the crystal lattice and chiral ligands on the surface. Compared with conventional perovskites possessing a single chiral origin, perovskites with multiple chirality theoretically offer the following advantages: (i) when different chiral sources respond to the same spectral region, their superposition is expected to yield a more pronounced chiral optical response; (ii) when the responsive spectral ranges of different chiral sources differ, their combination enables a broader spectral response; and (iii) the coexistence of multiple chiral origins implies the simultaneous presence of distinct chiral photovoltaic effects, the synergistic interaction of which may theoretically lead to significantly enhanced photovoltaic performance. The former two have been experimentally validated in terms of feasibility,[96] while their application in photovoltaics awaits future investigation. These promising attributes suggest that multi-chiral perovskite materials could emerge as a key research direction in the future development of chiral perovskites.

Challenges and prospects of chiral perovskite applications

Scalable synthesis of chiral perovskites: the premise of the application and promotion of the new materials is to achieve low-cost large-scale preparation. Although large-area preparation technology of achiral perovskite is relatively mature, low-cost large-area preparation of chiral perovskite is still a difficult problem because the volume of chiral molecules is generally large. In addition to the chiral nanostructures of perovskites, the synthesis methods of chiral perovskites can be mainly divided into the direct method and the chiral ligand-assisted method.[175] The former is mainly used to synthesize type I chiral perovskites whose chirality comes from internal ions of crystals, including cooling crystallization,[50,58,176] aqueous synthesis,[177] slow evaporation crystallization,[178] and antisolvent vapor-assisted crystallization (AVC).[74,179] The latter is mainly used to synthesize type II chiral perovskites with surface chiral ligands, including the single-step ultrasonication method,[180] the microwave-radiation-assisted method,[181] and so on. The preparation methods of perovskite chiral nanostructures can be divided into two categories: "bottom-up" and "top-down". The "bottom-up" synthesis method (e.g., nano-template method) is low cost, scalable, and uniform, but takes a long time, the chiral geometry is often not perfect, and the chirality is not significant. While

Please cite this article in press as: Feng et al., Chiral perovskites: From chirality mechanisms to photovoltaics, Matter (2026), https://doi.org/10.1016/j.matt.2026.102758

Table 4. Comparison of common synthesis methods for chiral perovskites

Methods		Cost	Chirality degree	Scalability	Crys.	Reference
Molecular chiral perovskite	cooling crystallization	low	CD: ≈140 mdeg (515 nm)[50]	high	microplate	Billing et al.[58]; Ahn et al.[176]; Ma et al.[50]
	aqueous synthesis	low	CD: ≈−50 mdeg (510 nm)	high	microplate	Wang et al.[177]
	slow evaporation crystallization	low	CD: ≈58 mdeg (203 nm)	high	microplate	Moon et al.[178]
	antisolvent vapor-assisted crystallization	low	CD: −0.14 mdeg/nm (405 nm)[179]	high	nanoplate	Yuan et al.[179]; Georgieva et al.[74]
	single-step ultrasonication method	low	glum: 7.0×10^{-3} (521 nm)	high	NC	Chen et al.[180]
	microwave-radiation-assisted method	low	CD: ≈–240 mdeg (247 nm)	high	NC	He et al.[181]
Perovskite chiral metamaterial	nano-template method	low	CD: ≈1,500 mdeg	high	–	Choi et al.[87]
	focused ion beam	high	CD: ≈6,350 mdeg (747 nm)	low	–	Long et al.[88]
	nanoimprinting method	low	glum: 0.16–0.31	high	–	Mendoza-Carreño et al.[89]

"top-down" manufacturing (e.g., nanoimprinting method and focused ion beam, FIB) shows more precise and high-resolution control in terms of the shape, size, and alignment of microstructures, it is costly and difficult to prepare large areas. The advantages and disadvantages of these methods are shown in Table 4. The nanoimprinting method, while exhibiting the strong chirality characteristic of top-down approaches, achieves considerable scalability through the reusability of templates, thereby positioning it as a promising candidate for the large-scale fabrication of perovskite chiral metamaterials. Furthermore, integrating "bottom-up" and "top-down" approaches (e.g., self-assembly combined with soft lithography) to combine the advantages of both represents another potential research direction.

Chirality to improve the stability of perovskite photovoltaics: although the conversion efficiency of perovskite solar cells, as the third generation of photovoltaic cells, has reached an impressive 27.3%,[38] poor stability and short life have always been important factors restricting the development of perovskite photovoltaic devices. High intensity and unstable light, humidity, oxygen, extreme temperatures, and mechanical stress can seriously affect the life of perovskite photovoltaic devices.[182–186] For a long time, the stability research of perovskite photovoltaic devices has been focused on light, temperature, oxygen, humidity, and other aspects, but ignored the influence of mechanical stress. Fortunately, recent studies have shown that the mechanical properties of perovskite solar cells can be effectively improved by introducing chiral molecules.[103] However, so far, the problem of a lack of stability and robustness of perovskite photovoltaic devices has not been completely solved, which is still the biggest obstacle to large-scale application of perovskite solar cells. Current studies[79,84] have proven that chiral perovskites can effectively improve the stability and extend the life of photovoltaic devices through passivation. Considering these studies alongside the improvement of the mechanical properties of perovskite solar cells by chiral molecules, it can be inferred that chirality may be a key that can help solve these problems.

Improvement of chiral perovskite photovoltaic conversion efficiency: the conversion efficiency of chiral perovskite photovoltaic devices has been paid much attention. On the one hand, as mentioned above, chiral perovskites shine in improving traditional photovoltaic performance. On the other hand, compared with mature classical photovoltaic devices, the conversion efficiency of the current novel photovoltaic devices based on chiral perovskites is small, which further restricts the improvement of current and power. The reason for the relatively small conversion efficiency may be that the band gap of perovskite material itself is wide, and the absorption of long wavelength light is weak. Additionally, it may be related to the lack of symmetry breaking of chiral perovskite materials. To solve this problem, one approach would be to develop new FE-PV materials and use energy band engineering to improve the photovoltaic performance of materials.[187] Another approach would be to strengthen the symmetry breaking of the materials to enhance its FE-PV effect (such as using perovskites with multiple mechanisms of chirality). The aforementioned strategy, being rooted in fundamental physics, entails considerable challenges. A more feasible approach is to extend strategies developed for conventional photovoltaics to FE-PVs based on chiral perovskites. Conventional tandem solar cells broaden the absorption spectrum and enhance power conversion efficiency by stacking subcells with different bandgaps (i.e., absorption spectra). Extending this strategy, chiral perovskite heterostructures with a bandgap gradient enable simultaneous absorption across different spectral ranges, thereby improving photovoltaic efficiency. Another method derived from conventional photovoltaics leverages the light-trapping effect of metamaterials[188] by incorporating light-trapping structures into FE-PV devices to achieve enhanced solar absorption.

Multi-functional materials and multi-characteristic coupling in perovskites: with the research and development of perovskite materials in recent years, chiral perovskites have been found to have many excellent properties, including optical chirality, polarity, ferroelectricity, pyroelectricity, and so on. This gives chiral perovskites a variety of applications. It has shown application potential in chiral optics, ferroelectrics, spin photonics, optoelectronics, photovoltaic power generation, and other fields. In addition, the interaction of a variety of excellent properties is expected to make breakthroughs in material

Please cite this article in press as: Feng et al., Chiral perovskites: From chirality mechanisms to photovoltaics, Matter (2026), https://doi.org/10.1016/j.matt.2026.102758

properties. Considering the diversity of chiral perovskite applications, multifunctional chiral perovskites began to receive attention. For example: chiral hybrid rare earth double perovskite [(R)/(S)-N-methyl-3-hydroxylquinu-clidinium]$_2$RbEu(NO$_3$)$_6$ has a good piezoelectric effect and CPLE[189]; another chiral hybrid rare earth perovskite, (R-N-methyl-3-hydroxylquinuclidinium)$_2$RbCe(NO$_3$)$_6$, was found to achieve both a piezoelectric response and piezomagnetic switching, and was the first time that the piezomagnetic switching was achieved in a molecular material.[190] In addition, $CsPbBr_3$ nanosheets modified with (R)/(S)-β-methylphenethylamine ligands exhibit both CD and CPLE.[81] Compared with traditional devices, devices designed and manufactured based on multifunctional materials can achieve more functions in a limited space, and have significant potential in the field of miniaturization and integration. The combination of various properties in chiral perovskites has also made breakthroughs. For example, the chiral and polar photovoltaic effect of chiral alternating cationic interspersed perovskite (R/S-PPA)EAPbCl$_4$ (EA = ethylammonium, PPA = 1-phenylpropylamine) shows the potential of self-powered shortwave ultraviolet circularly polarized light detection.[191] 2D chiral-polar double perovskite S/R-[(4-aminophenyl)ethylamine]$_2$AgBiI$_8$·0.5H$_2$O combines chiral optical phenomena and thermoluminescence electron effects to achieve unprecedented pyroelectric-based circularly polarized light detection.[192] In addition, studies have shown that the internal electric field of ferroelectrics can be used to inhibit carrier recombination and improve the efficiency of perovskite solar cells, which is called the ferroelectric coupling effect.[193] Although the ferroelectrics used in this study are not perovskite materials, and the ferroelectric materials are independent of the photovoltaic materials, it can be inferred that chiral perovskite ferroelectrics can simultaneously act as ferroelectric materials and photovoltaic materials to achieve the same ferroelectric coupling effect. Similarly, some studies have found that the combination of the FE-PV effect and classical photoelectric effect can also enhance the photovoltaic effect.[194] In summary, the current study shows that multi-characteristic coupling helps to strengthen the properties of materials (including photovoltaic properties) and will be a new possible direction for the development of chiral perovskite materials.

Other challenges and prospects

In addition to the problems mentioned above, the imperfection of chiral photovoltaic theory is also an important factor restricting the development of chiral perovskite photovoltaics. While CISS is believed to improve the performance of photovoltaic devices by improving carrier transport, there is still no perfect theoretical model to explain CISS itself. Although the volume photovoltaic effect model based on time-dependent perturbation theory has been rather accurate, the model based on Floquet theory and combined with the non-equilibrium Green's function (NEGF) method proposed in recent years seems to be more suitable when the light field is strong.[135,195–197] In addition, although many chiral perovskite materials show ferroelectricity and BPVEs, the question of how chirality affects the BPVE and depolarization field still lacks an answer based on a rigorous theoretical model. The imperfection of the theoretical model has hindered the further development of chiral perovskite photovoltaic devices to a great extent.

Green perovskite is an important focus of perovskite research. At present, the B-site ions of common halide perovskite materials are mostly lead ions with toxicity, which brings hidden dangers to human health and environmental safety. Therefore, it is particularly important to develop green perovskite materials that do not contain lead. In the field of chiral perovskites, one approach has been to use Bi,[142,144,198,199] Sn,[102,200–202] Ag,[144,199,203] Mn,[45] Sb,[204] Fe,[203] In,[203] Na,[203] and other low and non-toxic metal elements to replace Pb. Additionally, research on metal-free perovskite materials using ammonium ion as a B-site ion has also achieved results.[54] Although most of the current halide perovskites contain lead, as more lead-free perovskite materials are developed, safer and more reliable green perovskites will become alternative materials.

CONCLUSION

This paper reviews and divides the main mechanisms of chirality in perovskites into three categories: (I) internal ions of crystals; (II) surface chiral ligands; and (III) chiral nanostructures. The first two (I and II) can provide chirality by the ion/ligand's intrinsic chirality (if any), induced lattice distortion, and electron interaction, while the latter (III) achieves chirality by subwavelength geometric design. On this basis, we also discuss the mechanisms of chirality that cannot be classified into these three types, and propose the concept of "multiple mechanisms of chirality in perovskites," which exhibits significant theoretical potential in the fields of strongly optically chiral materials and broadband chiral optical response materials. Moreover, by integrating different chiral photovoltaic effects, such as the Rashba effect and CISS, it could provide a promising new route for enhancing photovoltaic performance.

Then, the potential of various chiral perovskites in photovoltaics is divided into two categories of discussion. For classical photovoltaics, the Rashba effect of type (I) chiral perovskites, the passivation and CISS of type (II) chiral perovskites can effectively inhibit carrier coupling and improve photovoltaic performance. In addition, type (I) chiral perovskites have also been found to strengthen mechanical properties of perovskite photovoltaics. For FE-PVs as novel photovoltaics, the depolarization field and BPVE fully demonstrate the potential of type (I) chiral perovskites. In addition, based on type (I) and (III) chiral perovskites, we propose "artificial ferroelectric domain walls based on chiral perovskites." Although not yet proven, by designing the chirality of perovskite materials, it may be possible to flexibly regulate ferroelectric domain walls, thereby achieving smarter and more pronounced FE-PV effects.

Finally, the challenges and prospects of chiral perovskite development and photovoltaic applications are discussed in categories, and possible research directions for the future are analyzed. It is hoped that this paper can serve as a helpful reference for future research.

ACKNOWLEDGMENTS

This work is supported partially by the National Natural Science Foundation of China (grant nos. 62405088, 52232008, 52102245, 52402254, and 22409061);

the Beijing Natural Science Foundation (Z240024, 2222076, and 2222077); the project of China Three Gorges Corporation named "key technologies of intelligent joint regulation and operation with grid connected friendly in power station group of wind, solar photovoltaic, and energy storage" (WWKY-2021-0173); Huaneng Group Headquarters Science and Technology Project (HNKJ20-H88); the Fundamental Research Funds for the Central Universities (2023MS042, 2023MS047, 2024MS036, and 2024MS039); and the NCEPU "Double First-Class" Program.

AUTHOR CONTRIBUTIONS

The authors confirm their contributions to the paper as follows: study conception and design were performed by M.L. and Y.F.; Y.F. developed the methodology; validation, formal analysis, data curation, and visualization were conducted by Y.Z., with assistance from X.B. and Y.D. in validation and data curation; investigation was carried out by X.B., Y.D., H.W., Y.W., J.L., F.Z., Z.W., C.Z., and C.J.; Q.Z. provided resources; project administration and funding acquisition were managed by Y.F.; the original draft was written by Y.Z.; and Y.F. together with C.A.N. reviewed and edited the manuscript; overall supervision was provided by M.L. and Y.F. All authors have reviewed and approved the final version of the manuscript.

DECLARATION OF INTERESTS

The authors declare no competing interests.

REFERENCES

1. Maes, J., Balcaen, L., Drijvers, E., Zhao, Q., De Roo, J., Vantomme, A., Vanhaecke, F., Geiregat, P., and Hens, Z. (2018). Light absorption coefficient of CsPbBr3 perovskite nanocrystals. J. Phys. Chem. Lett. *9*, 3093–3097.
2. Im, J.-H., Lee, C.-R., Lee, J.-W., Park, S.-W., and Park, N.-G. (2011). 6.5% efficient perovskite quantum-dot-sensitized solar cell. Nanoscale *3*, 4088–4093.
3. Qiu, X., Cao, B., Yuan, S., Chen, X., Qiu, Z., Jiang, Y., Ye, Q., Wang, H., Zeng, H., Liu, J., and Kanatzidis, M.G. (2017). From unstable CsSnI3 to air-stable Cs2SnI6: A lead-free perovskite solar cell light absorber with bandgap of 1.48 eV and high absorption coefficient. Sol. Energy Mater. Sol. Cell. *159*, 227–234.
4. Milot, R.L., Sutton, R.J., Eperon, G.E., Haghighirad, A.A., Martinez Hardigree, J., Miranda, L., Snaith, H.J., Johnston, M.B., and Herz, L.M. (2016). Charge-carrier dynamics in 2D hybrid metal–halide perovskites. Nano Lett. *16*, 7001–7007.
5. Senanayak, S.P., Yang, B., Thomas, T.H., Giesbrecht, N., Huang, W., Gann, E., Nair, B., Goedel, K., Guha, S., Moya, X., et al. (2017). Understanding charge transport in lead iodide perovskite thin-film field-effect transistors. Sci. Adv. *3*, e1601935.
6. Kagan, C.R., Mitzi, D.B., and Dimitrakopoulos, C.D. (1999). Organic-inorganic hybrid materials as semiconducting channels in thin-film field-effect transistors. Science *286*, 945–947.
7. Brenner, T.M., Egger, D.A., Kronik, L., Hodes, G., and Cahen, D. (2016). Hybrid organic—inorganic perovskites: low-cost semiconductors with intriguing charge-transport properties. Nat. Rev. Mater. *1*, 15007.
8. Stranks, S.D., Eperon, G.E., Grancini, G., Menelaou, C., Alcocer, M.J.P., Leijtens, T., Herz, L.M., Petrozza, A., and Snaith, H.J. (2013). Electron-hole diffusion lengths exceeding 1 micrometer in an organometal trihalide perovskite absorber. Science *342*, 341–344.
9. Xing, G., Mathews, N., Sun, S., Lim, S.S., Lam, Y.M., Grätzel, M., Mhaisalkar, S., and Sum, T.C. (2013). Long-range balanced electron-and hole-transport lengths in organic-inorganic CH3NH3PbI3. Science *342*, 344–347.
10. Dong, Q., Fang, Y., Shao, Y., Mulligan, P., Qiu, J., Cao, L., and Huang, J. (2015). Electron-hole diffusion lengths> 175 μm in solution-grown CH3NH3PbI3 single crystals. Science *347*, 967–970.
11. Chakraborty, R., Rajput, P.K., Anilkumar, G.M., Maqbool, S., Das, R., Rahman, A., Mandal, P., and Nag, A. (2023). Rational Design of Non-Centrosymmetric Hybrid Halide Perovskites. J. Am. Chem. Soc. *145*, 1378–1388. https://doi.org/10.1021/jacs.2c12034.
12. Fu, C., Gu, Z., Tang, Y., Xiao, Q., Zhang, S., Zhang, Y., and Song, Y. (2022). From structural design to functional construction: amine molecules in high-performance formamidinium-based perovskite solar cells. Angew. Chem. Int. Ed. Engl. *61*, e202117067.
13. Bhalla, A.S., Guo, R., and Roy, R. (2000). The perovskite structure—a review of its role in ceramic science and technology. Mater. Res. Innov. *4*, 3–26.
14. Hu, Z., Lin, Z., Su, J., Zhang, J., Chang, J., and Hao, Y. (2019). A review on energy band-gap engineering for perovskite photovoltaics. Sol. RRL *3*, 1970116.
15. Ergen, O., Gilbert, S.M., Pham, T., Turner, S.J., Tan, M.T.Z., Worsley, M.A., and Zettl, A. (2017). Graded bandgap perovskite solar cells. Nat. Mater. *16*, 522–525.
16. Chen, G., Li, P., Xue, T., Su, M., Ma, J., Zhang, Y., Wu, T., Han, L., Aldamasy, M., Li, M., et al. (2021). Design of low bandgap CsPb1− xSnxI2Br perovskite solar cells with excellent phase stability. Small *17*, 2101380.
17. Yang, T.C.-J., Fiala, P., Jeangros, Q., and Ballif, C. (2018). High-bandgap perovskite materials for multijunction solar cells. Joule *2*, 1421–1436.
18. Zhao, D., Chen, C., Wang, C., Junda, M.M., Song, Z., Grice, C.R., Yu, Y., Li, C., Subedi, B., Podraza, N.J., et al. (2018). Efficient two-terminal all-perovskite tandem solar cells enabled by high-quality low-bandgap absorber layers. Nat. Energy *3*, 1093–1100.
19. Rong, Y., Hu, Y., Mei, A., Tan, H., Saidaminov, M.I., Seok, S.I., McGehee, M.D., Sargent, E.H., and Han, H. (2018). Challenges for commercializing perovskite solar cells. Science *361*, eaat8235.
20. Green, M.A., Ho-Baillie, A., and Snaith, H.J. (2014). The emergence of perovskite solar cells. Nat. Photonics *8*, 506–514.
21. Correa-Baena, J.-P., Saliba, M., Buonassisi, T., Grätzel, M., Abate, A., Tress, W., and Hagfeldt, A. (2017). Promises and challenges of perovskite solar cells. Science *358*, 739–744.
22. Kim, J.Y., Lee, J.-W., Jung, H.S., Shin, H., and Park, N.-G. (2020). High-efficiency perovskite solar cells. Chem. Rev. *120*, 7867–7918.
23. Cui, P., Wei, D., Ji, J., Huang, H., Jia, E., Dou, S., Wang, T., Wang, W., and Li, M. (2019). Planar p–n homojunction perovskite solar cells with efficiency exceeding 21.3. Nat. Energy *4*, 150–159.
24. Qu, S., Huang, H., Wang, J., Cui, P., Li, Y., Wang, M., Li, L., Yang, F., Sun, C., Zhang, Q., et al. (2025). Revealing and Inhibiting the Facet-related Ion Migration for Efficient and Stable Perovskite Solar Cells. Angew. Chem. *64*, e202415949.
25. Yuan, M., Quan, L.N., Comin, R., Walters, G., Sabatini, R., Voznyy, O., Hoogland, S., Zhao, Y., Beauregard, E.M., Kanjanaboos, P., et al. (2016). Perovskite energy funnels for efficient light-emitting diodes. Nat. Nanotechnol. *11*, 872–877.
26. Wang, N., Cheng, L., Ge, R., Zhang, S., Miao, Y., Zou, W., Yi, C., Sun, Y., Cao, Y., Yang, R., et al. (2016). Perovskite light-emitting diodes based on solution-processed self-organized multiple quantum wells. Nat. Photonics *10*, 699–704.
27. Zhao, B., Bai, S., Kim, V., Lamboll, R., Shivanna, R., Auras, F., Richter, J.M., Yang, L., Dai, L., Alsari, M., et al. (2018). High-efficiency perovskite–polymer bulk heterostructure light-emitting diodes. Nat. Photonics *12*, 783–789.
28. Lin, K., Xing, J., Quan, L.N., de Arquer, F.P.G., Gong, X., Lu, J., Xie, L., Zhao, W., Zhang, D., Yan, C., et al. (2018). Perovskite light-emitting diodes with external quantum efficiency exceeding 20 per cent. Nature *562*, 245–248.
29. Zhang, K., Zhu, N., Zhang, M., Wang, L., and Xing, J. (2021). Opportunities and challenges in perovskite LED commercialization. J. Mater. Chem. C Mater. *9*, 3795–3799.

30. Pacchioni, G. (2021). Highly efficient perovskite LEDs. Nat. Rev. Mater. *6*, 108.
31. Fakharuddin, A., Gangishetty, M.K., Abdi-Jalebi, M., Chin, S.-H., bin Mohd Yusoff, A.R., Congreve, D.N., Tress, W., Deschler, F., Vasilopoulou, M., and Bolink, H.J. (2022). Perovskite light-emitting diodes. Nat. Electron. *5*, 203–216.
32. Liu, D., Hu, Z., Hu, W., Wangyang, P., Yu, K., Wen, M., Zu, Z., Liu, J., Wang, M., and Chen, W. (2017). Two-step method for preparing all-inorganic CsPbBr3 perovskite film and its photoelectric detection application. Mater. Lett. *186*, 243–246.
33. Wang, D., and Li, G. (2022). Advances in photoelectric detection units for imaging based on perovskite materials. Laser Photon. Rev. *16*, 2100713.
34. Li, C., Ma, Y., Xiao, Y., Shen, L., and Ding, L. (2020). Advances in perovskite photodetectors. InfoMat *2*, 1247–1256.
35. Sutherland, B.R., and Sargent, E.H. (2016). Perovskite photonic sources. Nat. Photonics *10*, 295–302.
36. Zhang, Q., Su, R., Du, W., Liu, X., Zhao, L., Ha, S.T., and Xiong, Q. (2017). Advances in small perovskite-based lasers. Small Methods *1*, 1700163.
37. Stylianakis, M.M., Maksudov, T., Panagiotopoulos, A., Kakavelakis, G., and Petridis, K. (2019). Inorganic and hybrid perovskite based laser devices: a review. Materials *12*, 859.
38. Green, M.A., Dunlop, E.D., Yoshita, M., Kopidakis, N., Bothe, K., Siefer, G., Hao, X., and Jiang, J. (2025). Solar Cell Efficiency Tables (Version 66). Progress in Photovoltaics. *33*, 795–810. https://doi.org/10.1002/pip.3919.
39. Lininger, A., Palermo, G., Guglielmelli, A., Nicoletta, G., Goel, M., Hinczewski, M., and Strangi, G. (2023). Chirality in light–matter interaction. Adv. Mater. *35*, 2107325.
40. Gal, J. (2008). The discovery of biological enantioselectivity: Louis Pasteur and the fermentation of tartaric acid, 1857—a review and analysis 150 yr later. Chirality *20*, 5–19.
41. Vargesson, N. (2015). Thalidomide-induced teratogenesis: History and mechanisms. Birth Defects Res. C Embryo Today. *105*, 140–156.
42. Ma, S., Ahn, J., and Moon, J. (2021). Chiral perovskites for next-generation photonics: from chirality transfer to chiroptical activity. Adv. Mater. *33*, 2005760.
43. Long, G., Sabatini, R., Saidaminov, M.I., Lakhwani, G., Rasmita, A., Liu, X., Sargent, E.H., and Gao, W. (2020). Chiral-perovskite optoelectronics. Nat. Rev. Mater. *5*, 423–439. https://doi.org/10.1038/s41578-020-0181-5.
44. Yang, C.-K., Chen, W.-N., Ding, Y.-T., Wang, J., Rao, Y., Liao, W.-Q., Tang, Y.-Y., Li, P.-F., Wang, Z.-X., and Xiong, R.-G. (2019). The First 2D Homochiral Lead Iodide Perovskite Ferroelectrics: [R- and S-1-(4-Chlorophenyl)ethylammonium]2PbI4. Adv. Mater. *31*, 1808088. https://doi.org/10.1002/adma.201808088.
45. Ai, Y., Chen, X.-G., Shi, P.-P., Tang, Y.-Y., Li, P.-F., Liao, W.-Q., and Xiong, R.-G. (2019). Fluorine Substitution Induced High Tc of Enantiomeric Perovskite Ferroelectrics: (R)- and (S)-3-(Fluoropyrrolidinium)MnCl3. J. Am. Chem. Soc. *141*, 4474–4479. https://doi.org/10.1021/jacs.9b00886.
46. Tang, Y.-Y., Ai, Y., Liao, W.-Q., Li, P.-F., Wang, Z.-X., and Xiong, R.-G. (2019). H/F-Substitution-Induced Homochirality for Designing High-Tc Molecular Perovskite Ferroelectrics. Adv. Mater. *31*, 1902163. https://doi.org/10.1002/adma.201902163.
47. Abendroth, J.M., Stemer, D.M., Bloom, B.P., Roy, P., Naaman, R., Waldeck, D.H., Weiss, P.S., and Mondal, P.C. (2019). Spin selectivity in photoinduced charge-transfer mediated by chiral molecules. ACS Nano *13*, 4928–4946.
48. Naaman, R., Paltiel, Y., and Waldeck, D.H. (2019). Chiral molecules and the electron spin. Nat. Rev. Chem *3*, 250–260.
49. Chen, C., Gao, L., Gao, W., Ge, C., Du, X., Li, Z., Yang, Y., Niu, G., and Tang, J. (2019). Circularly polarized light detection using chiral hybrid perovskite. Nat. Commun. *10*, 1927.
50. Ma, J., Fang, C., Chen, C., Jin, L., Wang, J., Wang, S., Tang, J., and Li, D. (2019). Chiral 2D perovskites with a high degree of circularly polarized photoluminescence. ACS Nano *13*, 3659–3665.
51. Lee, H., Lee, C.U., Yun, J., Jeong, C.-S., Jeong, W., Son, J., Park, Y.S., Moon, S., Lee, S., Kim, J.H., and Moon, J. (2024). A dual spin-controlled chiral two-/three-dimensional perovskite artificial leaf for efficient overall photoelectrochemical water splitting. Nat. Commun. *15*, 4672. https://doi.org/10.1038/s41467-024-49216-x.
52. Duan, T., and Zhou, Y. (2023). Leveraging Hierarchical Chirality in Perovskite (-Inspired) Halides for Transformative Device Applications. Adv. Energy Mater. *13*, 2200792.
53. Sohncke, L. (1879). Entwickelung einer Theorie der Krystallstruktur (BG Teubner).
54. Ye, H.-Y., Tang, Y.-Y., Li, P.-F., Liao, W.-Q., Gao, J.-X., Hua, X.-N., Cai, H., Shi, P.-P., You, Y.-M., and Xiong, R.-G. (2018). Metal-free three-dimensional perovskite ferroelectrics. Science *361*, 151–155.
55. Bai, J., Wang, H., Ma, J., Zhao, Y., Lu, H., Zhang, Y., Gull, S., Qiao, T., Qin, W., Chen, Y., et al. (2024). Wafer-Scale Patterning Integration of Chiral 3D Perovskite Single Crystals toward High-Performance Full-Stokes Polarimeter. J. Am. Chem. Soc. *146*, 18771–18780. https://doi.org/10.1021/jacs.4c06822.
56. Guan, Q., Zhu, T., Zhu, Z.K., Ye, H., You, S., Xu, P., Wu, J., Niu, X., Zhang, C., Liu, X., and Luo, J. (2023). Unprecedented chiral three-dimensional hybrid organic-inorganic perovskitoids. Angew. Chem. Int. Ed. Engl. *62*, e202307034.
57. Billing, D.G., and Lemmerer, A. (2003). Bis [(S)-β-phenethylammonium] tribromoplumbate (II). Acta Crystallogr., Sect. E: Struct. Rep. Online *59*, m381–m383.
58. Billing, D.G., and Lemmerer, A. (2006). Synthesis and crystal structures of inorganic–organic hybrids incorporating an aromatic amine with a chiral functional group. CrystEngComm *8*, 686–695.
59. Cao, Z., He, J., Jiao, C., Liu, Z., Xu, L., Zheng, C., Peng, S., and Chen, B. (2023). Chiroptical Activity in All-Inorganic Intrinsically Chiral Perovskite-like Nanocrystals Synthesized via Enantioselective Strategy. J. Phys. Chem. Lett. *14*, 2533–2541. https://doi.org/10.1021/acs.jpclett.3c00425.
60. Long, G., Zhou, Y., Zhang, M., Sabatini, R., Rasmita, A., Huang, L., Lakhwani, G., and Gao, W. (2019). Theoretical Prediction of Chiral 3D Hybrid Organic–Inorganic Perovskites. Adv. Mater. *31*, e1807628. https://doi.org/10.1002/adma.201807628.
61. Wang, L., Hao, W., Chen, S., Ren, J., and Li, H. (2025). Chiral 3D Perovskite Single Crystals Realized by Lattice Expansion. Adv. Sci. *12*, e06902.
62. Saparov, B., and Mitzi, D.B. (2016). Organic–inorganic perovskites: structural versatility for functional materials design. Chem. Rev. *116*, 4558–4596.
63. Long, G., Jiang, C., Sabatini, R., Yang, Z., Wei, M., Quan, L.N., Liang, Q., Rasmita, A., Askerka, M., Walters, G., et al. (2018). Spin control in reduced-dimensional chiral perovskites. Nat. Photonics *12*, 528–533. https://doi.org/10.1038/s41566-018-0220-6.
64. Han, S., Zhang, J., Sun, Z., Ji, C., Zhang, W., Wang, Y., Tao, K., Teng, B., and Luo, J. (2017). Lead-free hybrid material with an exceptional dielectric phase transition induced by a chair-to-boat conformation change of the organic cation. Inorg. Chem. *56*, 13078–13085.
65. Deng, W.-F., Li, Y.-X., Zhao, Y.-X., Hu, J.-S., Yao, Z.-S., and Tao, J. (2023). Inversion of Molecular Chirality Associated with Ferroelectric Switching in a High-Temperature Two-Dimensional Perovskite Ferroelectric. J. Am. Chem. Soc. *145*, 5545–5552. https://doi.org/10.1021/jacs.3c00634.
66. Hirotsu, S. (1977). Jahn-Teller induced phase transition in CsCuCl3: structural phase transition with helical atomic displacements. J. Phys. C Solid State Phys. *10*, 967–985.

67. Quintano, M., Moura, R.T., and Kraka, E. (2024). Exploring Jahn-Teller distortions: a local vibrational mode perspective. J. Mol. Model. *30*, 102. https://doi.org/10.1007/s00894-024-05882-8.

68. Kühne, I.A., Barker, A., Zhang, F., Stamenov, P., O'Doherty, O., Müller-Bunz, H., Stein, M., Rodriguez, B.J., and Morgan, G.G. (2020). Modulation of Jahn–Teller distortion and electromechanical response in a Mn3+ spin crossover complex. J. Phys. Condens. Matter *32*, 404002.

69. Gui, D., Ji, L., Muhammad, A., Li, W., Cai, W., Li, Y., Li, X., Wu, X., and Lu, P. (2018). Jahn–Teller Effect on Framework Flexibility of Hybrid Organic–Inorganic Perovskites. J. Phys. Chem. Lett. *9*, 751–755. https://doi.org/10.1021/acs.jpclett.7b03229.

70. Li, C., Lu, X., Ding, W., Feng, L., Gao, Y., and Guo, Z. (2008). Formability of ABX3 (X = F, Cl, Br, I) halide perovskites. Acta Crystallogr. Sect. B Struct. Sci. *64*, 702–707. https://doi.org/10.1107/s0108768108032734.

71. Tidrow, S.C. (2014). Mapping Comparison of Goldschmidt's Tolerance Factor with Perovskite Structural Conditions. Ferroelectrics *470*, 13–27. https://doi.org/10.1080/00150193.2014.922372.

72. Kim, Y.H., Song, R., Hao, J., Zhai, Y., Yan, L., Moot, T., Palmstrom, A.F., Brunecky, R., You, W., Berry, J.J., et al. (2022). The structural origin of chiroptical properties in perovskite nanocrystals with chiral organic ligands. Adv. Funct. Mater. *32*, 2200454.

73. Jiang, S., Song, Y., Kang, H., Li, B., Yang, K., Xing, G., Yu, Y., Li, S., Zhao, P., and Zhang, T. (2022). Ligand exchange strategy to achieve chiral perovskite nanocrystals with a high photoluminescence quantum yield and regulation of the chiroptical property. ACS Appl. Mater. Interfaces *14*, 3385–3394.

74. Georgieva, Z.N., Bloom, B.P., Ghosh, S., and Waldeck, D.H. (2018). Imprinting Chirality onto the Electronic States of Colloidal Perovskite Nanoplatelets. Adv. Mater. *30*, 1800097. https://doi.org/10.1002/adma.201800097.

75. Debnath, G.H., Georgieva, Z.N., Bloom, B.P., Tan, S., and Waldeck, D.H. (2021). Using post-synthetic ligand modification to imprint chirality onto the electronic states of cesium lead bromide (CsPbBr 3) perovskite nanoparticles. Nanoscale *13*, 15248–15256.

76. Forde, A., Ghosh, D., Kilin, D., Evans, A.C., Tretiak, S., and Neukirch, A.J. (2022). Induced Chirality in Halide Perovskite Clusters through Surface Chemistry. J. Phys. Chem. Lett. *13*, 686–693. https://doi.org/10.1021/acs.jpclett.1c04060.

77. Jin, X., Zhou, M., Han, J., Li, B., Zhang, T., Jiang, S., and Duan, P. (2022). A new strategy to achieve enhanced upconverted circularly polarized luminescence in chiral perovskite nanocrystals. Nano Res. *15*, 1047–1053.

78. Heindl, M.W., Kodalle, T., Fehn, N., Reb, L.K., Liu, S., Harder, C., Abdelsamie, M., Eyre, L., Sharp, I.D., Roth, S.V., et al. (2022). Strong Induced Circular Dichroism in a Hybrid Lead-Halide Semiconductor Using Chiral Amino Acids for Crystallite Surface Functionalization. Adv. Opt. Mater. *10*, 2200204.

79. Liu, J., He, J., Ma, D., He, J., and Wu, W. (2023). Chiral molecular environment determining selective coordination of cysteine to perovskite halogen vacancies. Sol. RRL *7*, 2200935.

80. Tran, T.K.T., Adewuyi, J.A., Wang, Y., Morales-Acosta, M.D., Mani, T., Ung, G., and Zhao, J. (2023). Anionic ligand-induced chirality in perovskite nanoplatelets. Chem. Commun. *59*, 1485–1488. https://doi.org/10.1039/d2cc05469h.

81. Cao, Q., Song, R., Chan, C.C.S., Wang, Z., Wong, P.Y., Wong, K.S., Blum, V., and Lu, H. (2023). Chiral Perovskite Nanoplatelets with Tunable Circularly Polarized Luminescence in the Strong Confinement Regime. Adv. Opt. Mater. *11*, 2203125. https://doi.org/10.1002/adom.202203125.

82. Ye, C., Jiang, J., Zou, S., Mi, W., and Xiao, Y. (2022). Core–Shell Three-Dimensional Perovskite Nanocrystals with Chiral-Induced Spin Selectivity for Room-Temperature Spin Light-Emitting Diodes. J. Am. Chem. Soc. *144*, 9707–9714. https://doi.org/10.1021/jacs.2c01214.

83. Jang, G., Jo, D.Y., Ma, S., Lee, J., Son, J., Lee, C.U., Jeong, W., Yang, S., Park, J.H., Yang, H., and Moon, J. (2024). Core–Shell Perovskite Quantum Dots for Highly Selective Room-Temperature Spin Light-Emitting Diodes. Adv. Mater. *36*, e2309335. https://doi.org/10.1002/adma.202309335.

84. Wu, W., Chen, Q., Cao, J., Fu, J., Zhang, Z., Chen, L., Rui, D., Zhang, J., Zhou, Y., and Song, B. (2024). Chirality-Induced Crystallization and Defect Passivation of Perovskites: Toward High-Performance Solar Cells. ACS Appl. Mater. Interfaces *16*, 16340–16350. https://doi.org/10.1021/acsami.4c01246.

85. Shi, Y., Duan, P., Huo, S., Li, Y., and Liu, M. (2018). Endowing perovskite nanocrystals with circularly polarized luminescence. Adv. Mater. *30*, 1705011.

86. Tepliakov, N.V., Vovk, I.A., Shlykov, A.I., Leonov, M.Y., Baranov, A.V., Fedorov, A.V., and Rukhlenko, I.D. (2019). Optical Activity and Circular Dichroism of Perovskite Quantum-Dot Molecules. J. Phys. Chem. C *123*, 2658–2664. https://doi.org/10.1021/acs.jpcc.8b12041.

87. Choi, Y.-J., Lee, J.-J., Park, J.-S., Kang, H., Kim, M., Kim, J., Okada, D., Kim, D.H., Araoka, F., and Choi, S.-W. (2024). Circularly Polarized Light Emission from Nonchiral Perovskites Incorporated into Nanoporous Cholesteric Polymer Templates. ACS Nano *18*, 909–918. https://doi.org/10.1021/acsnano.3c09596.

88. Long, G., Adamo, G., Tian, J., Klein, M., Krishnamoorthy, H.N.S., Feltri, E., Wang, H., and Soci, C. (2022). Perovskite metasurfaces with large superstructural chirality. Nat. Commun. *13*, 1551. https://doi.org/10.1038/s41467-022-29253-0.

89. Mendoza-Carreño, J., Molet, P., Otero-Martínez, C., Alonso, M.I., Polavarapu, L., and Mihi, A. (2023). Nanoimprinted 2D-Chiral Perovskite Nanocrystal Metasurfaces for Circularly Polarized Photoluminescence. Adv. Mater. *35*, 2210477. https://doi.org/10.1002/adma.202210477.

90. Cao, R., Yang, X., Wang, Y., and Xiao, Y. (2022). Induced circularly polarized luminescence of perovskite nanocrystals by self-assembly chiral gel. Nano Res. *16*, 1459–1464. https://doi.org/10.1007/s12274-022-4652-4.

91. Wang, K., Xing, G., Song, Q., and Xiao, S. (2021). Micro- and Nanostructured Lead Halide Perovskites: From Materials to Integrations and Devices. Adv. Mater. *33*, e2000306. https://doi.org/10.1002/adma.202000306.

92. Feng, Y., Leiderer, P., Zhao, R., Xiao, X., Giannini, V., Maier, S.A., Nemitz, C.A., Lin, Z., Ding, N., Kang, G., et al. (2020). Giant polarization anisotropic optical response from anodic aluminum oxide templates embedded with plasmonic metamaterials. Opt. Express *28*, 29513–29528.

93. Feng, Y., Kim, K.-D., Nemitz, C.A., Kim, P., Pfadler, T., Gerigk, M., Polarz, S., Dorman, J.A., Weickert, J., and Schmidt-Mende, L. (2016). Uniform large-area free-standing silver nanowire arrays on transparent conducting substrates. J. Electrochem. Soc. *163*, D447–D452.

94. Zhu, T., Bie, J., Ji, C., Zhang, X., Li, L., Liu, X., Huang, X.-Y., Fa, W., Chen, S., and Luo, J. (2022). Circular polarized light-dependent anomalous photovoltaic effect from achiral hybrid perovskites. Nat. Commun. *13*, 7702. https://doi.org/10.1038/s41467-022-35441-9.

95. Chen, G., Liu, X., An, J., Wang, S., Zhao, X., Gu, Z., Yuan, C., Xu, X., Bao, J., Hu, H.-S., et al. (2023). Nucleation-mediated growth of chiral 3D organic–inorganic perovskite single crystals. Nat. Chem. *15*, 1581–1590.

96. Zhao, Y., Askarpour, A.N., Sun, L., Shi, J., Li, X., and Alù, A. (2017). Chirality detection of enantiomers using twisted optical metamaterials. Nat. Commun. *8*, 14180. https://doi.org/10.1038/ncomms14180.

97. Zhou, Q., and Chen, J. (2025). Meticulous Design of Chiral Molecules in Efficient and Stable Perovskite Solar Cells. Adv. Funct. Mater. *35*, 2502139. https://doi.org/10.1002/adfm.202502139.

98. Rashba, E., and Sheka, V. (2015). Symmetry of energy bands in crystals of wurtzite type II. In Symmetry of bands with spin-orbit interaction included.

99. Zhai, Y., Baniya, S., Zhang, C., Li, J., Haney, P., Sheng, C.-X., Ehrenfreund, E., and Vardeny, Z.V. (2017). Giant Rashba splitting in 2D

organic-inorganic halide perovskites measured by transient spectroscopies. Sci. Adv. *3*, e1700704. https://doi.org/10.1126/sciadv.1700704.

100. Niesner, D., Wilhelm, M., Levchuk, I., Osvet, A., Shrestha, S., Batentschuk, M., Brabec, C., and Fauster, T. (2016). Giant Rashba Splitting in-CH3NH3PbBr3Organic-Inorganic Perovskite. Phys. Rev. Lett. *117*, 126401. https://doi.org/10.1103/PhysRevLett.117.126401.

101. Zheng, F., Tan, L.Z., Liu, S., and Rappe, A.M. (2015). Rashba Spin–Orbit Coupling Enhanced Carrier Lifetime in CH3NH3PbI3. Nano Lett. *15*, 7794–7800. https://doi.org/10.1021/acs.nanolett.5b01854.

102. Gao, W., Dong, H., Sun, N., Chao, L., Hui, W., Wei, Q., Li, H., Xia, Y., Gao, X., Xing, G., et al. (2022). Chiral cation promoted interfacial charge extraction for efficient tin-based perovskite solar cells. J. Energy Chem. *68*, 789–796. https://doi.org/10.1016/j.jechem.2021.09.019.

103. Duan, T., You, S., Chen, M., Yu, W., Li, Y., Guo, P., Berry, J.J., Luther, J.M., Zhu, K., and Zhou, Y. (2024). Chiral-structured heterointerfaces enable durable perovskite solar cells. Science *384*, 878–884. https://doi.org/10.1126/science.ado5172.

104. Kepenekian, M., Robles, R., Katan, C., Sapori, D., Pedesseau, L., and Even, J. (2015). Rashba and Dresselhaus effects in hybrid organic–inorganic perovskites: from basics to devices. ACS Nano *9*, 11557–11567.

105. Jana, M.K., Song, R., Liu, H., Khanal, D.R., Janke, S.M., Zhao, R., Liu, C., Valy Vardeny, Z., Blum, V., and Mitzi, D.B. (2020). Organic-to-inorganic structural chirality transfer in a 2D hybrid perovskite and impact on Rashba-Dresselhaus spin-orbit coupling. Nat. Commun. *11*, 4699. https://doi.org/10.1038/s41467-020-18485-7.

106. Li, J., Guo, Z., Qin, Y., Liu, R., He, Y., Zhu, X., Xu, F., and He, T. (2023). Rashba Effect and Spin-Dependent Excitonic Properties in Chiral Two-Dimensional/Three-Dimensional Composite Perovskite Films. J. Phys. Chem. Lett. *14*, 11697–11703. https://doi.org/10.1021/acs.jpclett.3c03247.

107. Lee, T.-D., and Yang, C.-N. (1956). Question of parity conservation in weak interactions. Phys. Rev. *104*, 254–258.

108. Ray, K., Ananthavel, S., Waldeck, D., and Naaman, R. (1999). Asymmetric scattering of polarized electrons by organized organic films of chiral molecules. Science *283*, 814–816.

109. Göhler, B., Hamelbeck, V., Markus, T.Z., Kettner, M., Hanne, G.F., Vager, Z., Naaman, R., and Zacharias, H. (2011). Spin selectivity in electron transmission through self-assembled monolayers of double-stranded DNA. Science *331*, 894–897.

110. Naaman, R., and Waldeck, D.H. (2012). Chiral-Induced Spin Selectivity Effect. J. Phys. Chem. Lett. *3*, 2178–2187. https://doi.org/10.1021/jz300793y.

111. Bloom, B.P., Paltiel, Y., Naaman, R., and Waldeck, D.H. (2024). Chiral Induced Spin Selectivity. Chem. Rev. *124*, 1950–1991. https://doi.org/10.1021/acs.chemrev.3c00661.

112. Yan, L., Huang, H., Cui, P., Du, S., Lan, Z., Yang, Y., Qu, S., Wang, X., Zhang, Q., Liu, B., et al. (2023). Fabrication of perovskite solar cells in ambient air by blocking perovskite hydration with guanabenz acetate salt. Nat. Energy *8*, 1158–1167.

113. Wang, X., Huang, H., Wang, M., Lan, Z., Cui, P., Du, S., Yang, Y., Yan, L., Zhang, Q., Qu, S., and Li, M. (2024). Oriented molecular bridge constructs homogeneous buried interface for perovskite solar cells with efficiency over 25.3%. Adv. Mater. *36*, 2310710.

114. Du, S., Huang, H., Lan, Z., Cui, P., Li, L., Wang, M., Qu, S., Yan, L., Sun, C., Yang, Y., et al. (2024). Inhibiting perovskite decomposition by a creeper-inspired strategy enables efficient and stable perovskite solar cells. Nat. Commun. *15*, 5223.

115. He, L., Zhang, Y., Wei, Y., Cai, Y., Zhang, J., and Wang, P. (2023). A helicene-based semiconducting polymer for stable and efficient perovskite solar cells. Matter *6*, 4013–4031. https://doi.org/10.1016/j.matt.2023.09.006.

116. Li, Z., Xie, T., Wang, C., Chen, Z., Li, D., Wang, Q., Shi, B., Huang, S., Zheng, F., and Chi, D. (2025). Interfacial molecular engineering with p-F-MBAI achieves 22.43% efficiency and exceptional stability in wide-bandgap perovskite solar cells. Chem. Eng. J. *519*, 165441. https://doi.org/10.1016/j.cej.2025.165441.

117. Li, X., Dong, X., Shen, Z., Zai, X., Li, Y., Miao, Z., Song, L., and Wu, Z. (2025). Halogenated Chiral Organic Spacer Cation Regulation for Efficient and Stable 2D Ruddlesden-Popper Perovskite Solar Cells. Adv. Funct. Mater. *35*, 2507591. https://doi.org/10.1002/adfm.202507591.

118. Cejas-Sánchez, J. (2025). Chiral aza-helicene-based tandem solar cells. Nat. Synth. *4*, 1022. https://doi.org/10.1038/s44160-025-00888-3.

119. Liu, T., Li, C., Li, Y., Saliba, M., Cheng, H.-M., and Wang, Z. (2024). Chiral materials meet perovskite solar cells. Green Carbon *2*, 405–406.

120. Gao, J.-X., Zhang, W.-Y., Wu, Z.-G., Zheng, Y.-X., and Fu, D.-W. (2020). Enantiomorphic Perovskite Ferroelectrics with Circularly Polarized Luminescence. J. Am. Chem. Soc. *142*, 4756–4761. https://doi.org/10.1021/jacs.9b13291.

121. Hu, Y., Florio, F., Chen, Z., Phelan, W.A., Siegler, M.A., Zhou, Z., Guo, Y., Hawks, R., Jiang, J., Feng, J., et al. (2020). A chiral switchable photovoltaic ferroelectric 1D perovskite. Sci. Adv. *6*, eaay4213. https://doi.org/10.1126/sciadv.aay4213.

122. Li, L.-S., Tan, Y.-H., Wei, W.-J., Gao, H.-Q., Tang, Y.-Z., and Han, X.-B. (2021). Chiral Switchable Low-Dimensional Perovskite Ferroelectrics. ACS Appl. Mater. Interfaces *13*, 2044–2051. https://doi.org/10.1021/acsami.0c19507.

123. Fu, D., Hou, Z., He, Y., Liu, J.-C., Lv, H.-P., and Tang, Y.-Y. (2022). Multiaxial Ferroelectricity and Ferroelasticity in a Chiral Perovskite. Chem. Mater. *34*, 3518–3524. https://doi.org/10.1021/acs.chemmater.2c00546.

124. Zeng, Y.-L., Huang, X.-Q., Huang, C.-R., Zhang, H., Wang, F., and Wang, Z.-X. (2021). Unprecedented 2D Homochiral Hybrid Lead-Iodide Perovskite Thermochromic Ferroelectrics with Ferroelastic Switching. Angew. Chem. Int. Ed. Engl. *60*, 10730–10735. https://doi.org/10.1002/anie.202102195.

125. Fan, C.-C., Han, X.-B., Liang, B.-D., Shi, C., Miao, L.-P., Chai, C.-Y., Liu, C.-D., Ye, Q., and Zhang, W. (2022). Chiral Rashba Ferroelectrics for Circularly Polarized Light Detection. Adv. Mater. *34*, 2204119. https://doi.org/10.1002/adma.202204119.

126. Sui Li, L., Juan Wei, W., Qiang Gao, H., Hui Tan, Y., and Bo Han, X. (2021). Molecular Disorder Induces an Unusual Phase Transition in a Potential 2D Chiral Ferroelectric Perovskite. Chemistry *27*, 9054–9059. https://doi.org/10.1002/chem.202100334.

127. Matsuo, H., and Noguchi, Y. (2024). Bulk photovoltaic effect in ferroelectrics. Jpn. J. Appl. Phys. *63*, 060101. https://doi.org/10.35848/1347-4065/ad442e.

128. Belinicher, V.I., and Sturman, B.I. (1980). The photogalvanic effect in media lacking a center of symmetry. Sov. Phys. Usp. *23*, 199–223.

129. Lines, M.E., and Glass, A.M. (2001). Principles and Applications of Ferroelectrics and Related Materials (Oxford university press).

130. Fridkin, V.M. (2001). Bulk photovoltaic effect in noncentrosymmetric crystals. Crystallogr. Rep. *46*, 654–658.

131. Belinicher, V., Malinovskiĭ, V., and Sturman, B. (1977). Photogalvanic effect in a crystal with polar axis. Soviet J. Exp. Theor. Phys. *46*, 362.

132. Fridkin, V. Applications of Ferroelectrics held jointly with 2012 European Conference on the Applications of Polar Dielectrics and 2012 International Symp Piezoresponse Force Microscopy and Nanoscale Phenomena in Polar Materials (ISAF/ECAPD/PFM), 2012 Intl Symp, 2012. .

133. Butler, K.T., Frost, J.M., and Walsh, A. (2015). Ferroelectric materials for solar energy conversion: photoferroics revisited. Energy Environ. Sci. *8*, 838–848. https://doi.org/10.1039/c4ee03523b.

134. Sturman, B.I. (2020). Ballistic and shift currents in the bulk photovoltaic effect theory. Phys. Usp. *63*, 407–411. https://doi.org/10.3367/UFNe.2019.06.038578.

135. Dai, Z., and Rappe, A.M. (2023). Recent progress in the theory of bulk photovoltaic effect. Chem. Phys. Rev. *4*, 011303. https://doi.org/10.1063/5.0101513.

136. Young, S.M., and Rappe, A.M. (2012). First Principles Calculation of the Shift Current Photovoltaic Effect in Ferroelectrics. Phys. Rev. Lett. *109*, 116601. https://doi.org/10.1103/PhysRevLett.109.116601.

137. Dai, Z., Schankler, A.M., Gao, L., Tan, L.Z., and Rappe, A.M. (2021). Phonon-assisted ballistic current from first-principles calculations. Phys. Rev. Lett. *126*, 177403.

138. Dai, Z., and Rappe, A.M. (2021). First-principles calculation of ballistic current from electron-hole interaction. Phys. Rev. B *104*, 235203.

139. Noma, T., Chen, H.Y., Dhara, B., Sotome, M., Nomoto, T., Arita, R., Nakamura, M., and Miyajima, D. (2023). Bulk Photovoltaic Effect Along the Nonpolar Axis in Organic-Inorganic Hybrid Perovskites. Angew. Chem. Int. Ed. Engl. *62*, e202309055. https://doi.org/10.1002/anie.202309055.

140. Huang, P.-J., Taniguchi, K., and Miyasaka, H. (2019). Bulk Photovoltaic Effect in a Pair of Chiral–Polar Layered Perovskite-Type Lead Iodides Altered by Chirality of Organic Cations. J. Am. Chem. Soc. *141*, 14520–14523. https://doi.org/10.1021/jacs.9b06815.

141. Ye, H., Peng, Y., Wei, M., Zhang, X., Zhu, T., Guan, Q., Li, L., Chen, S., Liu, X., and Luo, J. (2023). Bulk Photovoltaic Effect in Chiral Layered Hybrid Perovskite Enables Highly Sensitive Near-Infrared Circular Polarization Photodetection. Chem. Mater. *35*, 6591–6597. https://doi.org/10.1021/acs.chemmater.2c03770.

142. You, S., Zhu, Z.K., Dai, S., Wu, J., Guan, Q., Zhu, T., Yu, P., Chen, C., Chen, Q., and Luo, J. (2023). Inch-Size Single Crystals of Lead-Free Chiral Perovskites with Bulk Photovoltaic Effect for Stable Self-Driven X-Ray Detection. Adv. Funct. Mater. *33*, 2303523. https://doi.org/10.1002/adfm.202303523.

143. Huang, P.-J., Taniguchi, K., and Miyasaka, H. (2022). Crucial Contribution of Polarity for the Bulk Photovoltaic Effect in a Series of Noncentrosymmetric Two-Dimensional Organic–Inorganic Hybrid Perovskites. Chem. Mater. *34*, 4428–4436. https://doi.org/10.1021/acs.chemmater.2c00094.

144. Li, D., Liu, X., Wu, W., Peng, Y., Zhao, S., Li, L., Hong, M., and Luo, J. (2021). Chiral Lead-Free Hybrid Perovskites for Self-Powered Circularly Polarized Light Detection. Angew. Chem. Int. Ed. Engl. *60*, 8415–8418. https://doi.org/10.1002/anie.202013947.

145. Ishii, A., Sone, R., Yamada, T., Noto, M., Suzuki, H., Nakamura, D., Murata, K., Shiga, T., Ishii, K., and Nihei, M. (2025). Giant Bulk Photovoltaic Effect in a Chiral Polar Crystal based on Helical One-dimensional Lead Halide Perovskites. Angew. Chem. Int. Ed. Engl. *64*, e202424391. https://doi.org/10.1002/anie.202424391.

146. Meyer, B., and Vanderbilt, D. (2002). Ab initiostudy of ferroelectric domain walls inPbTiO3. Phys. Rev. B *65*, 104111. https://doi.org/10.1103/PhysRevB.65.104111.

147. Yang, S.Y., Seidel, J., Byrnes, S.J., Shafer, P., Yang, C.H., Rossell, M.D., Yu, P., Chu, Y.H., Scott, J.F., Ager, J.W., et al. (2010). Above-bandgap voltages from ferroelectric photovoltaic devices. Nat. Nanotechnol. *5*, 143–147. https://doi.org/10.1038/nnano.2009.451.

148. Kang, S.H., Shan, S., Noorduin, W.L., Khan, M., Aizenberg, J., and Bertoldi, K. (2013). Buckling-Induced Reversible Symmetry Breaking and Amplification of Chirality Using Supported Cellular Structures. Adv. Mater. *25*, 3380–3385. https://doi.org/10.1002/adma.201300617.

149. Seidel, J., Martin, L.W., He, Q., Zhan, Q., Chu, Y.H., Rother, A., Hawkridge, M.E., Maksymovych, P., Yu, P., Gajek, M., et al. (2009). Conduction at domain walls in oxide multiferroics. Nat. Mater. *8*, 229–234. https://doi.org/10.1038/nmat2373.

150. Yang, D., Jin, L., Martinez, R.V., Bertoldi, K., Whitesides, G.M., and Suo, Z. (2016). Phase-transforming and switchable metamaterials. Extreme Mech. Lett. *6*, 1–9.

151. Raney, J.R., Nadkarni, N., Daraio, C., Kochmann, D.M., Lewis, J.A., and Bertoldi, K. (2016). Stable propagation of mechanical signals in soft media using stored elastic energy. Proc. Natl. Acad. Sci. USA *113*, 9722–9727.

152. Frazier, M.J., and Kochmann, D.M. (2017). Atomimetic mechanical structures with nonlinear topological domain evolution kinetics. Adv. Mater. *29*, 1605800.

153. Jin, L., Khajehtourian, R., Mueller, J., Rafsanjani, A., Tournat, V., Bertoldi, K., and Kochmann, D.M. (2020). Guided transition waves in multistable mechanical metamaterials. Proc. Natl. Acad. Sci. USA *117*, 2319–2325.

154. Paulose, J., Meeussen, A.S., and Vitelli, V. (2015). Selective buckling via states of self-stress in topological metamaterials. Proc. Natl. Acad. Sci. USA *112*, 7639–7644.

155. Xia, X., Afshar, A., Yang, H., Portela, C.M., Kochmann, D.M., Di Leo, C.V., and Greer, J.R. (2019). Electrochemically reconfigurable architected materials. Nature *573*, 205–213.

156. Rafsanjani, A., Jin, L., Deng, B., and Bertoldi, K. (2019). Propagation of pop ups in kirigami shells. Proc. Natl. Acad. Sci. USA *116*, 8200–8205.

157. Yasuda, H., Korpas, L.M., and Raney, J.R. (2020). Transition waves and formation of domain walls in multistable mechanical metamaterials. Phys. Rev. Appl. *13*, 054067.

158. Deng, B., Yu, S., Forte, A.E., Tournat, V., and Bertoldi, K. (2020). Characterization, stability, and application of domain walls in flexible mechanical metamaterials. Proc. Natl. Acad. Sci. USA *117*, 31002–31009. https://doi.org/10.1073/pnas.2015847117.

159. Jia, Q.-Q., Zhang, Z.-X., Ni, H.-F., Lin, Q., Teri, G., Liu, P.-G., Luo, J.-Q., Huang, P.-Z., Wang, Z.-J., Wang, C.-F., et al. (2025). Polarization-Switching Controlled Luminescence in Hybrid Ferroelectric. Angew. Chem. Int. Ed. Engl. *64*, e202505163. https://doi.org/10.1002/anie.202505163.

160. Jia, Q.-Q., Teri, G., Zhou, Q.-F., Luo, J.-Q., Ni, H.-F., Huang, P.-Z., Liu, P.-G., Pan, L., Wang, C.-F., Liu, Z., et al. (2025). Two-Dimensional Heterovalent Alloying Hybrid Double Perovskite Solid Solution for Elevating Ferroelastic Photoelectric Response. Angew. Chem. Int. Ed. Engl. *64*, e202514669. https://doi.org/10.1002/anie.202514669.

161. Li, C., Telychko, M., Zheng, Y., Yuan, S., Wu, Z., Wong, W.P.D., Li, Y., Jin, Y., Io, W.F., Wang, X., et al. (2024). Switchable planar chirality and spin texture in highly ordered ferroelectric hybrid perovskite domains. Nat. Commun. *15*, 10221.

162. Li, Y., Jin, Y., and Leng, K. (2025). Ferroelectric Domains and Domain Walls in Organic–Inorganic Hybrid Perovskites. Chem. Mater. *37*, 4935–4943.

163. Zhang, L., Jiang, J., Multunas, C., Ming, C., Chen, Z., Hu, Y., Lu, Z., Pendse, S., Jia, R., Chandra, M., et al. (2022). Room-temperature electrically switchable spin–valley coupling in a van der Waals ferroelectric halide perovskite with persistent spin helix. Nat. Photonics *16*, 529–537.

164. Chynoweth, A.G. (1956). Surface space-charge layers in barium titanate. Phys. Rev. *102*, 705–714.

165. Setter, N., Damjanovic, D., Eng, L., Fox, G., Gevorgian, S., Hong, S., Kingon, A., Kohlstedt, H., Park, N.Y., Stephenson, G.B., et al. (2006). Ferroelectric thin films: Review of materials, properties, and applications. J. Appl. Phys. *100*, 051606.

166. Mehta, R.R., Silverman, B.D., and Jacobs, J.T. (1973). Depolarization fields in thin ferroelectric films. J. Appl. Phys. *44*, 3379–3385.

167. Glinchuk, M.D., Eliseev, E.A., and Stephanovich, V.A. (2002). The depolarization field effect on the thin ferroelectric films properties. Phys. B Condens. Matter *322*, 356–370.

168. Black, C.T., Farrell, C., and Licata, T.J. (1997). Suppression of ferroelectric polarization by an adjustable depolarization field. Appl. Phys. Lett. *71*, 2041–2043. https://doi.org/10.1063/1.119781.

169. Griffiths, D.J. (2023). Introduction to Electrodynamics (Cambridge University Press).

170. Su, W., Li, X., Li, L., Yang, D., Wang, F., Wei, X., Zhou, W., Kataura, H., Xie, S., and Liu, H. (2023). Chirality-dependent electrical transport

properties of carbon nanotubes obtained by experimental measurement. Nat. Commun. *14*, 1672. https://doi.org/10.1038/s41467-023-37443-7.

171. Kwon, D.-H., Werner, P.L., and Werner, D.H. (2008). Optical planar chiral metamaterial designs for strong circular dichroism and polarization rotation. Opt. Express *16*, 11802–11807.
172. Ma, W., Cheng, F., and Liu, Y. (2018). Deep-learning-enabled on-demand design of chiral metamaterials. ACS Nano *12*, 6326–6334.
173. Luo, C., Sang, T., Ge, Z., Lu, J., and Wang, Y. (2024). Flexible design of chiroptical response of planar chiral metamaterials using deep learning. Opt. Express *32*, 13978–13985. https://doi.org/10.1364/oe.510656.
174. Liu, Q., Wei, Q., Ren, H., Zhou, L., Zhou, Y., Wang, P., Wang, C., Yin, J., and Li, M. (2023). Circular polarization-resolved ultraviolet photonic artificial synapse based on chiral perovskite. Nat. Commun. *14*, 7179. https://doi.org/10.1038/s41467-023-43034-3.
175. Ma, J., Wang, H., and Li, D. (2021). Recent Progress of Chiral Perovskites: Materials, Synthesis, and Properties. Adv. Mater. *33*, e2008785. https://doi.org/10.1002/adma.202008785.
176. Ahn, J., Lee, E., Tan, J., Yang, W., Kim, B., and Moon, J. (2017). A new class of chiral semiconductors: chiral-organic-molecule-incorporating organic–inorganic hybrid perovskites. Mater. Horiz. *4*, 851–856.
177. Wang, J., Fang, C., Ma, J., Wang, S., Jin, L., Li, W., and Li, D. (2019). Aqueous synthesis of low-dimensional lead halide perovskites for room-temperature circularly polarized light emission and detection. ACS Nano *13*, 9473–9481.
178. Moon, T.H., Oh, S.-J., and Ok, K.M. (2018). [((R)-C8H12N) 4] [Bi2Br10] and [((S)-C8H12N) 4] [Bi2Br10]: chiral hybrid bismuth bromides templated by chiral organic cations. ACS Omega *3*, 17895–17903.
179. Yuan, C., Li, X., Semin, S., Feng, Y., Rasing, T., and Xu, J. (2018). Chiral lead halide perovskite nanowires for second-order nonlinear optics. Nano Lett. *18*, 5411–5417.
180. Chen, W., Zhang, S., Zhou, M., Zhao, T., Qin, X., Liu, X., Liu, M., and Duan, P. (2019). Two-photon absorption-based upconverted circularly polarized luminescence generated in chiral perovskite nanocrystals. J. Phys. Chem. Lett. *10*, 3290–3295.
181. He, T., Li, J., Li, X., Ren, C., Luo, Y., Zhao, F., Chen, R., Lin, X., and Zhang, J. (2017). Spectroscopic studies of chiral perovskite nanocrystals. Appl. Phys. Lett. *111*, 151102.
182. Wang, D., Wright, M., Elumalai, N.K., and Uddin, A. (2016). Stability of perovskite solar cells. Sol. Energy Mater. Sol. Cell. *147*, 255–275.
183. Boyd, C.C., Cheacharoen, R., Leijtens, T., and McGehee, M.D. (2019). Understanding degradation mechanisms and improving stability of perovskite photovoltaics. Chem. Rev. *119*, 3418–3451.
184. Zhu, H., Teale, S., Lintangpradipto, M.N., Mahesh, S., Chen, B., McGehee, M.D., Sargent, E.H., and Bakr, O.M. (2023). Long-term operating stability in perovskite photovoltaics. Nat. Rev. Mater. *8*, 569–586.
185. Kim, H.S., Seo, J.Y., and Park, N.G. (2016). Material and device stability in perovskite solar cells. ChemSusChem *9*, 2528–2540.
186. Meng, L., You, J., and Yang, Y. (2018). Addressing the stability issue of perovskite solar cells for commercial applications. Nat. Commun. *9*, 5265.
187. Aftab, S., Iqbal, M.Z., Haider, Z., Iqbal, M.W., Nazir, G., and Shehzad, M.A. (2022). Bulk Photovoltaic Effect in 2D Materials for Solar-Power Harvesting. Adv. Opt. Mater. *10*, 2201288. https://doi.org/10.1002/adom.202201288.
188. Wei, B., Mao, X., Liu, W., Ji, C., Yang, G., Bao, Y., Chen, X., Wei, S., and Wang, X. (2025). A metasurface light-trapping structure for solar cell applications. Opt. Express *33*, 858–866. https://doi.org/10.1364/OE.544821.
189. Wang, C.-F., Shi, C., Zheng, A., Wu, Y., Ye, L., Wang, N., Ye, H.-Y., Ju, M.-G., Duan, P., Wang, J., and Zhang, Y. (2022). Achieving circularly polarized luminescence and large piezoelectric response in hybrid rare-earth double perovskite by a chirality induction strategy. Mater. Horiz. *9*, 2450–2459. https://doi.org/10.1039/d2mh00698g.
190. Hu, Z.B., Wang, C.F., Sha, T.T., Shi, C., Ye, L., Ye, H.Y., Song, Y., You, Y.M., and Zhang, Y. (2022). An Effective Strategy of Introducing Chirality to Achieve Multifunctionality in Rare-Earth Double Perovskite Ferroelectrics. Small Methods *6*, e2200421. https://doi.org/10.1002/smtd.202200421.
191. Zhu, T., Wu, H., Ji, C., Zhang, X., Peng, Y., Yao, Y., Ye, H., Weng, W., Lin, W., and Luo, J. (2022). Polar Photovoltaic Effect in Chiral Alternating Cations Intercalation-Type Perovskites Driving Self-Powered Ultraviolet Circularly Polarized Light Detection. Adv. Opt. Mater. *10*, 2200146. https://doi.org/10.1002/adom.202200146.
192. Li, Z., Ji, C., Fan, Y., Zhu, T., You, S., Wu, J., Li, R., Zhu, Z.-K., Yu, P., Kuang, X., and Luo, J. (2023). Circularly Polarized Light-Dependent Pyro-Phototronic Effect from 2D Chiral–Polar Double Perovskites. J. Am. Chem. Soc. *145*, 25134–25142. https://doi.org/10.1021/jacs.3c05080.
193. Jia, E., Wei, D., Cui, P., Ji, J., Huang, H., Jiang, H., Dou, S., Li, M., Zhou, C., and Wang, W. (2019). Efficiency Enhancement with the Ferroelectric Coupling Effect Using P(VDF-TrFE) in CH3NH3PbI3 Solar Cells. Adv. Sci. *6*, 1900252. https://doi.org/10.1002/advs.201900252.
194. Zhang, J., Su, X., Shen, M., Dai, Z., Zhang, L., He, X., Cheng, W., Cao, M., and Zou, G. (2013). Enlarging photovoltaic effect: combination of classic photoelectric and ferroelectric photovoltaic effects. Sci. Rep. *3*, 2109. https://doi.org/10.1038/srep02109.
195. Morimoto, T., and Nagaosa, N. (2016). Topological nature of nonlinear optical effects in solids. Sci. Adv. *2*, e1501524.
196. Bajpai, U., Popescu, B.S., Plecháč, P., Nikolić, B.K., Foa Torres, L.E.F., Ishizuka, H., and Nagaosa, N. (2019). Spatio-temporal dynamics of shift current quantum pumping by femtosecond light pulse. J. Phys. Mater. *2*, 025004.
197. Ishizuka, H., and Nagaosa, N. (2017). Local photo-excitation of shift current in noncentrosymmetric systems. New J. Phys. *19*, 033015.
198. Zhong, W.-H., Chen, H.-R., Li, Z.-M., Zhu, J.-Y., Shi, C.-H., Cao, Q.-L., Zhao, J.-J., and Chen, L.-Z. (2023). 1D Chiral Enantiomer Lead-Free Perovskites Induced Chiralopical Activity and Photoelectric Response. Inorg. Chem. *62*, 17985–17992. https://doi.org/10.1021/acs.inorgchem.3c02994.
199. Zhu, Z.K., Zhu, T., Wu, J., You, S., Yu, P., Liu, X., Li, L., Ji, C., and Luo, J. (2023). Discovering New Type of Lead-Free Cluster-Based Hybrid Double Perovskite Derivatives with Chiral Optical Activities and Low X-Ray Detection Limit. Adv. Funct. Mater. *33*, 2214660. https://doi.org/10.1002/adfm.202214660.
200. Zhao, L., Han, X., Zheng, Y., Yu, M.-H., and Xu, J. (2021). Tin-based chiral perovskites with second-order nonlinear optical properties. Adv. Photon. Res. *2*, 2100056.
201. Lu, H., Xiao, C., Song, R., Li, T., Maughan, A.E., Levin, A., Brunecky, R., Berry, J.J., Mitzi, D.B., Blum, V., and Beard, M.C. (2020). Highly distorted chiral two-dimensional tin iodide perovskites for spin polarized charge transport. J. Am. Chem. Soc. *142*, 13030–13040.
202. Imran, T., Rauf, S., Raza, H., Aziz, L., Chen, R., Liu, S., Wang, J., Ahmad, M.A., Zhang, S., Zhang, Y., et al. (2022). Methylammonium and Bromide-Free Tin-Based Low Bandgap Perovskite Solar Cells. Adv. Energy Mater. *12*, 2200305. https://doi.org/10.1002/aenm.202200305.
203. Xue, J., Wang, Z., Comstock, A., Wang, Z., Sung, H.H.Y., Williams, I.D., Sun, D., Liu, J., and Lu, H. (2022). Chemical Control of Magnetic Ordering in Hybrid Fe–Cl Layered Double Perovskites. Chem. Mater. *34*, 2813–2823. https://doi.org/10.1021/acs.chemmater.2c00163.
204. Azmy, A., Konovalova, D.M., Lepore, L., Fyffe, A., Kim, D., Wojtas, L., Tu, Q., Trinh, M.T., Zibouche, N., and Spanopoulos, I. (2023). Synthesis and Optical Properties of One Year Air-Stable Chiral Sb(III) Halide Semiconductors. Inorg. Chem. *62*, 20142–20152. https://doi.org/10.1021/acs.inorgchem.3c03098.